POISONING THE INNER PREDICTION LOGIC OF GRAPH NEURAL NETWORKS FOR CLEAN-LABEL BACKDOOR ATTACKS

Anonymous authors
Paper under double-blind review

ABSTRACT

Graph Neural Networks (GNNs) have achieved remarkable results in various tasks. Recent studies reveal that graph backdoor attacks can poison the GNN model to predict test nodes with triggers attached as the target class. However, apart from injecting triggers to training nodes, these graph backdoor attacks generally require altering the labels of trigger-attached training nodes into the target class, which is impractical in real-world scenarios. In this work, we focus on the clean-label graph backdoor attack, a realistic but understudied topic where training labels are not modifiable. According to our preliminary analysis, existing graph backdoor attacks generally fail under the clean-label setting. Our further analysis identifies that the core failure of existing methods lies in their inability to poison the prediction logic of GNN models, leading to the triggers being deemed unimportant for prediction. Therefore, we study a novel problem of effective clean-label graph backdoor attacks by poisoning the inner prediction logic of GNN models. We propose **BA-LOGIC** to solve the problem by coordinating a poisoned node selector and a logic-poisoning trigger generator. Extensive experiments on real-world datasets demonstrate that our method effectively enhances the attack success rate and surpasses state-of-the-art graph backdoor attack competitors under clean-label settings. Our code is available at https://anonymous.4open.science/r/BA-Logic.

1 INTRODUCTION

Graph neural networks (GNNs) Kipf & Welling (2017); Veličković et al. (2018); Hamilton et al. (2017) have achieved promising results in diverse graph-based applications, such as social networks Ni et al. (2024), finance systems Cheng et al. (2022), and drug discovery Bongini et al. (2021). Most GNNs update the representation of a node by aggregating features from its neighbors with the message-passing mechanism. Thus, the representations learned by GNNs can preserve node features and neighbor topology, facilitating various graph representation learning tasks Xu et al. (2019).

Despite GNNs having achieved success, they are vulnerable to graph backdoor attacks Dai et al. (2023); Xi et al. (2021); Zhang et al. (2021). We illustrate the general process of existing graph backdoor attacks in Fig. 1. As Fig. 1 shows, to create a backdoored graph, the adversary will attach a selected set of poisoned nodes with *triggers*. In addition, the adversary will *alter labels* of the poisoned nodes to the target class regardless of their original classes. Then, the GNN model trained on this poisoned graph will learn to associate the presence of the trigger with the target class, resulting in a backdoored GNN model. During the inference phase, the backdoored GNN will misclassify test nodes attached with the trigger to the target class while maintaining regular prediction accuracy on clean nodes. Some initial efforts Dai et al. (2023); Xi et al. (2021); Zhang et al. (2021) have demonstrated the effectiveness of the graph backdoor attacks. For instance, SBA Zhang et al. (2021) conducts pioneering research on graph backdoor attacks by adopting randomly generated triggers. Building upon this work, GTA Xi et al. (2021) proposed a trigger generator to guarantee the effectiveness of graph backdoor attacks. The state-of-the-art method UGBA Dai et al. (2023) adopts an unnoticeable constraint into the trigger generator to make the attack more unnoticeable while maintaining a high attack success rate. More detailed discussion of related works is in Appendix D.

However, as the Fig. 1 illustrates, the majority of graph backdoor attacks, such as UGBA Dai et al. (2023) and DPGBA Zhang et al. (2024b), require attackers to alter the labels of trigger-attached poisoned nodes to the target class, regardless of their ground-truth labels. Such manipulation of the training labels is often impractical. In many application scenarios, the training set is annotated by experts of the dataset owners. It would be very expensive or even infeasible to manipulate the labels of the training set. For instance, fake account labels of Twitter are annotated and stored within a well-protected back-end system, making it nearly impossible for attackers to alter the labels Alothali et al. (2018). Furthermore, modifying labels of training samples can increase the risk of being detected. Therefore, it is crucial to investigate backdoor attacks under the clean-label setting. Specifically, as illustrated in Fig. 1, clean-label backdoor attackers inject triggers into training samples of the target class without modifying their labels, which is a more practical and challenging attack scenario. Some initial efforts Fan & Dai (2024); Xu & Picek (2022) have been conducted for clean-label graph backdoor attacks. For instance, Fan & Dai (2024) employs a single node as an efficient trigger, while Xu & Picek (2022) uses random graphs, respectively.

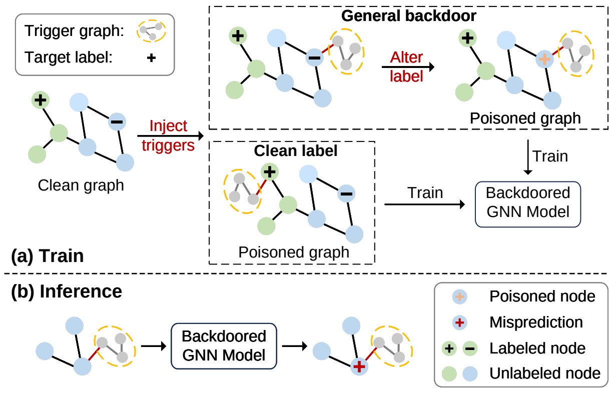

Figure 1: Illustration of graph backdoor attacks under both the general and clean-label settings.

Despite the state-of-the-art general graph backdoor methods and initial attempts at clean-label backdoor attacks, our preliminary analysis in Sec. 2.3 reveals that these methods often fail to effectively poison the decision logic of target GNN models, resulting in poor backdoor performance. More precisely, our experiments indicate that during the poisoning phase, for a training sample attached with the poisoning trigger, clean neighbors dominate the prediction of the target GNN model. By contrast, injected triggers would be treated as irrelevant information, resulting in poor backdoor attacks. In fact, under the clean-label setting, poisoned samples that are attached with triggers are correctly labeled with ground-truth labels (target class). Consequently, during the training phase, the GNN model naturally learn correct patterns associated with the labeled class, thus ignoring the injected triggers during prediction. To address this problem, it is promising for attackers to explicitly guide the model's inner prediction logic to emphasize the injected triggers when predicting the poisoned nodes. Though promising, the works on poisoning the inner logic of GNNs for clean-label backdoor attacks are rather limited.

Therefore, in this paper, we study a novel and essential problem of poisoning the inner logic of GNN models for effective clean-label graph backdoor attacks. In essence, we face two technical challenges: *Firstly*, how to obtain triggers capable of poisoning the inner prediction logic of target GNN models. *Secondly*, the budget for the number of triggers injected is generally limited, so how to fully leverage the budget of poisoned nodes for effective inner prediction logic poisoning. In an attempt to address these challenges, we propose a novel Clean-Label Graph Backdoor Attack by Inner Logic Poisoning (BA-LOGIC). BA-LOGIC employs a logic-poisoning trigger generator, guided by a novel prediction logic poisoning loss. To better utilize the budget of poisoned nodes, BA-LOGIC further employs a poisoned node selection module for logic poisoning. We summarize our contributions as follows:

- We study a novel problem of poisoning the inner prediction logic of target models for clean-label graph backdoor attacks;
- We introduce an innovative framework, BA-LOGIC, which is capable of optimizing the poisoned node set and generating logic-poisoning triggers for effective clean-label backdoor attacks;
- We conduct comprehensive experiments for diverse target GNN models across a wide range of real-world graph datasets. Consistent results unequivocally demonstrate the superiority of BA-LOGIC over state-of-the-art backdoor attacks. This substantiates the significant improvement in the effectiveness of clean-label graph backdoor attacks, achieved through the novel inner prediction logic poisoning strategy we present.

2 PRELIMINARIES

2.1 THREAT MODEL OF LOGIC POISONING FOR CLEAN-LABEL BACKDOOR ATTACKS

Notations A graph $\mathcal{G} = (\mathcal{V}, \mathcal{E})$ consists of a set of N nodes $\mathcal{V} = \{v_1, \ldots, v_N\}$ and edges $\mathcal{E}$. $\mathbf{A} \in \mathbb{R}^{N \times N}$ is the adjacency matrix and $\mathbf{X} \in \mathbb{R}^{N \times d}$ is the node feature matrix. This work focuses on an inductive node classification task, where only a subset of nodes $\mathcal{V}_L$ has assigned labels $\mathcal{Y}_L$ for training, and unlabeled nodes are denoted as $\mathcal{V}_U$. Test nodes $\mathcal{V}_T$ are unavailable during training.

Threat Model Attackers aims to inject backdoor triggers to a subset of training nodes $\mathcal{V}_P$, forcing the GNN f_θ trained on the poisoned graph to learn the backdoor patterns introduced by the trigger and misclassify the nodes in $\mathcal{V}_T$ that attached with trigger g as the target class y_t. Meanwhile, the backdoored GNN f_θ should maintain the accuracy on the clean test nodes with no trigger attached. In the clean-label graph backdoor attack, *attackers are not capable of altering the labels of nodes*. During training, attackers can only attach triggers to a subset of labeled nodes $\mathcal{V}_P \subset \mathcal{V}_L$ to poison the target model. During inference, attackers can only attach triggers to the target test nodes. Following Zhang et al. (2024b); Dai et al. (2023), the information about the target model, such as architectures and hyperparameters, is unavailable to attackers. Instead, attackers can only select a surrogate model to transfer the attack to unseen target models. This black-box threat model poses a strict limitation on the attacker. Threat model level comparison with existing works is in Appendix E.

2.2 LIMITATIONS OF EXISTING METHODS UNDER CLEAN-LABEL SETTING

To evaluate existing graph backdoor methods under clean-label setting, we employ three state-of-the-art graph backdoor methods, namely GTA Xi et al. (2021), UGBA Dai et al. (2023), and DPGBA Zhang et al. (2024b). We extend them to the clean-label setting and denote the extended methods as **GTA-C**, **UGBA-C**, and **DPGBA-C**, where **-C** indicates it as a variation for the clean-label setting that only poisons labeled nodes of the target class without altering their labels. We also include an initial effort of a clean-label backdoor attack **ERBA** Xu & Picek (2022), which injects Erdös-Rényi random graphs Erdos et al. (1960) to labeled nodes of the target class as triggers. We report the average attack success rate **(ASR)** and clean accuracy **(CA)** of 5 runs on **Pubmed** in Tab. 1. From the table, it is evident that (i) all the methods exhibit poor ASR with the number of poisoned nodes $\mathcal{V}_P$ set as 100; (ii) even with a larger $|\mathcal{V}_P|$, the ASR improves marginally. The results confirm the inadequacy of existing graph backdoor attacks under clean-label settings.

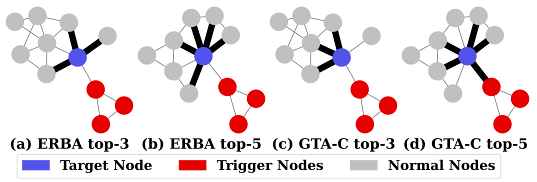

Figure 2: GNNExplainer's visualization of important subgraphs in a poisoned node's computational graph. We bold the edges connecting the poisoned node and the top-3 (a, c) and top-5 (b, d) most important nodes, respectively.

Table 1: ASR | CA (%) for GCN on Pubmed.

$\lvert\mathcal{V}_P\rvert$	ERBA	GTA-C	UGBA-C	DPGBA-C
100	22.2 | 85.6	38.4 | 85.1	71.1 | 85.3	64.2 | 85.2
200	22.5 | 85.2	38.9 | 85.0	71.2 | 85.1	64.1 | 85.1
300	23.0 | 85.0	38.7 | 85.2	71.2 | 84.8	64.2 | 84.7

Table 2: IRT (%) under clean-label setting.

Top-k	ERBA	GTA-C	UGBA-C	DPGBA-C
$k = 3$	12.3	21.0	42.4	33.8
$k = 5$	15.1	22.6	44.3	34.7

2.3 WHY EXISTING METHODS FALL SHORT?

To understand why existing methods fail under clean-label settings, we analyze the impact of injected triggers empirically and theoretically. By using GNNExplainer Ying et al. (2019) to extract edge/node masks as explanations, we visualize the prediction for a poisoned node classified as y_t in a GCN model backdoored by ERBA and GTA-C, showing subgraphs consisting of top-k important nodes in Fig. 2. Results reveal that triggers from both methods exhibit lower importance than poisoned nodes' clean neighbors, suggesting their limited influence on model predictions.

To further assess the injected triggers' influence on backdoored GNN predictions, we propose a metric named Important Rate of Triggers **(IRT)** to quantify trigger contributions by measuring their proportion as top-k critical nodes in compact graphs of poisoned nodes. The mathematical formulation is in Appendix H. Tab. 2 reports IRT values of existing methods on **Cora**, showing that the IRT values for subgraphs consisting of top-3 and top-5 important nodes remain low across all methods, indicating triggers are rarely critical for target class prediction. We further conduct a theoretical analysis to prove that the existing methods fail to poison the inner logic of the target model, resulting in poor ASR.

Assumptions on Graphs Following Dai et al. (2023); Zhang et al. (2025), we consider a graph $\mathcal{G}$ where (i) The node feature $\mathbf{x}_i \in \mathbb{R}^d$ is sampled from a specific feature distribution F_{y_i} that depends on the node label y_i. (ii) Dimensional features of $\mathbf{x}_i$ are independent to each other. (iii) The magnitude of node features is bounded by a positive scalar vector S, i.e., $\max_{i,j} |\mathbf{x}_i(j)| \leq S$.

Theorem 1. *We consider a graph $\mathcal{G} = (\mathcal{V}, \mathcal{E}, \mathbf{X})$ follows Assumptions. Given a node v_i with label y_i, let deg_i be the degree of v_i, and γ be the value of the important rate of trigger. For a node v_i attached with trigger g_i, the probability for GNN model f predict v_i as target class y_t is bounded by:*

$$\mathbb{P}(f(v_i) = y_t) \leq 2d \cdot \exp\left(-\frac{deg_i \cdot (1-\gamma)^2 \cdot \|\mu_{y_t} - \mu_{y_i}\|_2^2}{2d \cdot S^2}\right), \tag{1}$$

where d is the node feature dimension, μ_{y_t} and μ_{y_i} are the class centroid vectors in the feature space for y_i and y_t, respectively.

The detailed proof is in Appendix H. Theorem 1 shows that the upper bound of the probability for predicting the trigger-attached v_i as y_t grows with the increase in the IRT value γ. Existing graph backdoor methods generally lead to a low important rate of triggers, resulting in poor attack performance under the clean-label setting. The analysis further motivates a new graph backdoor paradigm that poisons the inner prediction logic of GNNs for effective clean-label graph backdoor attacks. More empirical analysis on IRT and attack budget $\mathcal{V}_P$ is in Appendix A.9, and more empirical validations on theoretical analysis are in Appendix J.

3 Problem Definition

We denote the prediction on a clean node v_i as $f_\theta(v_i) = f_\theta(\mathcal{G}_C^i)$, where $\mathcal{G}_C^i$ is the computational graph of node v_i. For a node v_i injected with trigger g_i, the prediction from the model is denoted as $f_\theta(\tilde{v}_i) = f_\theta(a(\mathcal{G}_C^i, g_i))$, where $a(\cdot)$ is the trigger attachment operation. Let $S_\theta(\tilde{v}_i, g_i)$ denote the importance score of the trigger g_i injected to the node v_i determined by the target GNN f_θ.

Our preliminary analysis in Sec. 2.3 shows that existing backdoor attacks suffer from a poor ASR under clean-label settings due to the failure to poison the inner logic of the target model. To effectively conduct clean-label graph backdoor attacks, we propose to generate triggers capable of poisoning the inner logic of the target model. More precisely, the proposed clean-label graph backdoor attacks aim to achieve the following objectives:

- For any node $v_i \in \mathcal{V}_P \cup \mathcal{V}_T$, after attachment with the generated trigger g_i, the backdoored GNN will classify v_i as the target class y_t, i.e., $f_\theta(\tilde{v}_i) = y_t$.
- For poisoned nodes and test nodes attached with triggers, injected triggers should be identified as the most important nodes by the logic of backdoored GNN, i.e., maximizing $S_\theta(\tilde{v}_i, g_i)$ for all node $v_i \in \mathcal{V}_P \cup \mathcal{V}_T$.
- Constraints, including the number of poisoned nodes, the size of generated triggers, and other unnoticeable constraints as the one outlined in Dai et al. (2023), should be met.

With the above objectives and the threat model discussed in Sec. 2.1, We can formulate the clean-label graph backdoor attack by poisoning the inner prediction logic as:

Problem 1. *Given a graph $\mathcal{G} = (\mathcal{V}, \mathcal{E})$ with a set of labeled training nodes $\mathcal{V}_L$ with labels $\mathcal{Y}_L$, we aim to learn a trigger generator f_g: $v_i \rightarrow g_i$ and select a set of nodes $\mathcal{V}_P \subset \mathcal{V}_L^t$ to attach logic-poisoning triggers so that a GNN model f trained on the poisoned graph will classify the test node attached with the trigger to the target class y_t by solving:*

$$\begin{aligned} \min_{\mathcal{V}_P, \theta_g} \quad & \sum_{v_i \in \mathcal{V}} l(f_{\theta^*}(\tilde{v}_i), y_t) - \beta S_{\theta^*}(v_i, g_i) \\ s.t. \quad & \theta^* = \arg\min_\theta \sum_{v_i \in \mathcal{V}_L \setminus \mathcal{V}_P} l(f_\theta(v_i), y_i) + \sum_{v_i \in \mathcal{V}_P} l(f_\theta(\tilde{v}_i), y_i), \\ & \forall v_i \in \mathcal{V}, g_i \textit{ meets the required unnoticeable constraint}, \quad |g_i| \leq \Delta_g, \quad |\mathcal{V}_P| \leq \Delta_P \end{aligned} \tag{2}$$

where θ_g denotes the parameters of the trigger generator, $l(\cdot)$ denotes the cross-entropy loss, and β is the hyperparameter to control the contribution of logic poisoning. The node size of the trigger $|g_i|$ is limited by Δ_g, and the number of poisoned nodes is limited by Δ_P. A surrogate GNN f is applied to simulate the target GNN whose architecture is unknown. Various unnoticeable constraints can be applied to this problem. In this paper, we focus on the unnoticeable constraint in Dai et al. (2023).

4 Methodology

Our preliminary analysis reveals two key challenges for logic poisoning clean-label graph backdoor attacks: (i) How to select the poisoned nodes that are most effective in logic poisoning? (ii) How to efficiently compute the objective function of prediction logic poisoning to guide the training of the clean-label backdoor trigger generator? To overcome the above challenges, we propose a novel method Ba-Logic, and illustrate the overall framework in Fig. 3.

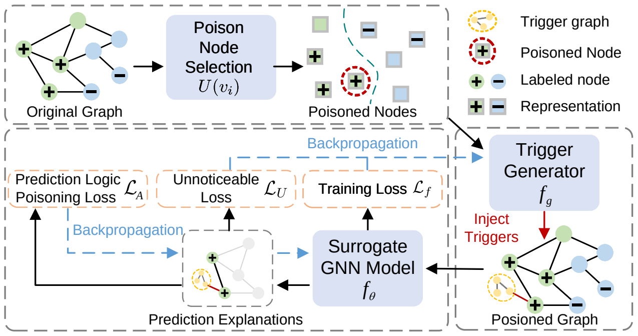

Figure 3: Framework of Ba-Logic.

As Fig. 3 shows, Ba-Logic firstly identifies poisoned nodes of the target class with high prediction uncertainty. The logic-poisoning trigger generator f_g utilizes node features as a basis to iteratively optimize triggers for the clean-label graph backdoor. To guide the training of the logic-poisoning trigger generator f_g, an efficient objective function for poisoning the prediction logic of the surrogate GNN model is employed. Additionally, to ensure the unnoticeability of triggers, a constraint is incorporated in the training of the trigger generator. Next, we give the details of each component.

4.1 Poisoned Node Selection for Clean-Label Backdoor Attacks

In this subsection, we present the details of the poisoned node selection. It indicates the optimal positions for trigger injection, after which the model trained on the trigger-injected graph is backdoored, and arbitrary test nodes could be successfully attacked by attaching triggers during inference.

The poisoned nodes are randomly selected in several existing clean-label graph backdoor methods Xu & Picek (2022); Xing et al. (2024), resulting in waste of the limited attack budget on useless poisoned nodes. For example, some labeled nodes exhibit typical patterns strongly associated with the target class. Thus, it would be difficult for the injected triggers to attain high importance scores with the presence of these typical patterns, thereby invalidating the backdoor trigger in logic poisoning.

Therefore, we design a process of identifying the set of poisoned nodes $\mathcal{V}_P \in \mathcal{V}_L^t$ that are most effective for backdoor. Specifically, we propose to select training nodes of the target class that exhibit high uncertainty as predicted by the clean GNN. Intuitively, high uncertainty indicates irregular patterns that are weakly associated with the target class y_t. By contrast, triggers obtained by the generator will exhibit consistent patterns to poison the prediction logic. Thus, when triggers are injected into such nodes, the model is more likely to treat these triggers as key features of the target class rather than irregular patterns. Specifically, to identify high uncertainty nodes, we utilize the output of a GCN trained on the clean graph $\mathcal{G}$ and label set $\mathcal{Y}_L$. Let f_S denote the well-trained GCN model, the probability of node v_i predicted as the class y_j can be obtained by:

$$p(y_j|v_i) = f_S(v_i)_{y_c} \tag{3}$$

Moreover, we design an uncertainty metric based on the following two aspects: (i) The probability that the node predicted as the target class, i.e., $p(y_j|v_i)$, should be low; (ii) The node is also expected to be uncertain for all other classes, i.e., the entropy of the probability vector is high. Let C be the number of classes. The score function of poisoned node selection for attacking logic is:

$$U(v_i) = (1 - p(y_t|v_i)) - \sum_{j=1}^{C} p(y_j|v_i) \log p(y_j|v_i) \tag{4}$$

After getting the score of each $v_i \in \mathcal{V}_L^t$, we select nodes with top-Δ_P highest scores to construct $\mathcal{V}_P$ that satisfies the attack budget.

4.2 Inner Prediction Logic Poisoning

With the poisoned nodes $\mathcal{V}_P$ selected for the clean-label backdoor attack, the backdoored graph to poison the target GNN can be constructed by inserting powerful logic-poisoning triggers. In this subsection, we introduce the design of the logic-poisoning trigger generator. Then, we present the objective function of prediction logic poisoning that guides the training of the trigger generator.

Logic-Poisoning Trigger Generator To poison the logic of the target GNN model, the generated trigger must be capable of capturing the importance scores for predictions on a poisoned node. Therefore, the logic-poisoning trigger should be adaptive to the input node. To achieve this, we deploy a MLP model to simultaneously generate node features and the adjacency of the trigger g_i for node v_i by:

$$\mathbf{X}_i^g,\ \ \mathbf{A}_i^g = \mathbf{MLP}\left(\mathbf{x}_i\right), \tag{5}$$

where $\mathbf{x}_i$ is the feature of node v_i. $\mathbf{X}_i^g \in \mathbb{R}^{s\times d}$ is the features of the trigger nodes, where s and d represent the size of the generated trigger and dimension of node features, respectively. $\mathbf{A}_i^g \in \mathbb{R}^{s\times s}$ represents the adjacency matrix of the generated trigger. As the adjacency matrix must be discrete, we deploy the updating strategy of discrete variables in a binarized neural network Hubara et al. (2016).

To build the backdoored graph dataset for model poisoning, the generated trigger $g_i = (\mathbf{X}_i^g, \mathbf{A}_i^g)$ will be attached to the corresponding poisoned node $v_i \in \mathcal{V}_P$. During the inference phase, to mislead the backdoored GNN to predict the test node $v_i \in \mathcal{V}_T$ as target class y_t, the attacker would insert the trigger generated by f_g.

The prediction logic poisoning in BA-LOGIC aims to mislead the target model to treat triggers as crucial patterns for prediction. As shown in Eq.(2), this can be formulated as maximizing the trigger's importance score $S_\theta(\tilde{v}_i, g_i)$ in predicting the trigger-attached node $v_i \in \mathcal{V}$ as the target class y_t by a surrogate GNN model f_θ. Although GNN explainers such as GNNExplainer Ying et al. (2019) and PGExplainer Luo et al. (2020) are capable of computing importance scores for nodes, they necessitate additional optimization to generate explanations. This extra optimization step poses challenges for solving Eq.(2), both in terms of computational cost and gradient backpropagation. Thus, BA-LOGIC deploys the gradient-based explanation, i.e., Sensitivity Analysis (SA) Baldassarre & Azizpour (2019). Specifically, for the prediction $\tilde{y}_i = f(\tilde{v}_i)$ on a trigger-attached node v_i, SA computes importance scores using the norm of the gradient w.r.t the node v_j. Formally, the important score of node v_j in predicting v_i as the target class is computed by:

$$S(y_i^t, v_j) = \|\frac{\partial \tilde{y}_i^c}{\partial \mathbf{x}_j}\|_2, \tag{6}$$

where y_i^c is score of predicting node v_i attached trigger g into the target class, and $\mathbf{x}_j$ represents the node features of v_j. The Eq.(6) will allow us the compute the importance scores of inserted triggers efficiently. Simply maximizing the importance scores of triggers as specified in Eq.(6) can lead to infinitely large gradients, which significantly degrade the utility of the target model. Alternatively, within the computational graph of a trigger-attached node v_i, BA-LOGIC enforces the importance scores of trigger nodes to exceed those of clean nodes by a predefined margin T. More precisely, we replace the term of maximizing importance scores of triggers in Eq.(2) with the following prediction logic poisoning loss:

$$\mathcal{L}_A = \sum_{v_i\in\mathcal{V}} \max\Big(0, T - \big(\sum_{v_g\in g_i} S(y_i^t, v_g) - \sum_{v_c\in\mathcal{N}(v_i)} S(y_i^t, v_c)\big)\Big), \tag{7}$$

where $\mathcal{N}(v_i)$ denotes the clean node net in the computational graph of the trigger-attached node v_i.

Unnoticeable Constraint on Triggers As we need to bypass various defense methods, an unnoticeable constraint on the generated trigger is required. Our BA-LOGIC is flexible to various types of unnoticeable constraints on triggers. Following Dai et al. (2023), we propose the constraint that requires high cosine similarity between the poisoned node or target node v_i and trigger g_i. Within the generated trigger g_i, the connected trigger nodes should also exhibit high similarity. Formally, the loss of an unnoticeable constraint on trigger generator f_g can be formulated as:

$$\min_{\theta_g} \mathcal{L}_U = \sum_{v_i\in\mathcal{V}} \sum_{(v_j,v_k)\in\mathcal{E}_B^i} \exp(-sim(v_j, v_k)), \tag{8}$$

where $\mathcal{E}_B^i$ denotes the edge set that contains edges insider trigger g_i and edges attaching trigger g_i and node v_i. $sim(\cdot)$ represents the computation of cosine similarity between vectors. The unnoticeable loss in Eq.(8) is applied on all nodes to guarantee that generated triggers meet the unnoticeable constraint on various nodes.

4.3 Final Objective Function of Ba-Logic

As it is stated in Eq.(2), a bi-level optimization between the logic-poisoning trigger generator f_g and a surrogate GNN model f is adopted to ensure the effectiveness of triggers in logic poisoning for the clean-label backdoor. In the lower-level optimization of Eq.(2), the surrogate GNN model is trained on the backdoored dataset by:

$$\min_{\theta} \mathcal{L}_f = \sum_{v_i \in \mathcal{V}_L \setminus \mathcal{V}_P} l(f_\theta(v_i), y_i) + \sum_{v_i \in \mathcal{V}_P} l(f_\theta(\tilde{v}_i), y_i) \tag{9}$$

The upper-level optimization in Eq.(2) aims for successful backdoor attacks and inner prediction logic poisoning. With the selected poisoned node set $\mathcal{V}_P$, the prediction logic poisoning loss $\mathcal{L}_A$ in Eq.(7), and the unnoticeable constraint $\mathcal{L}_U$ in Eq.(8), the optimization problem in Eq.(2) can be finally reformulated as:

$$\min_{\theta_g} \sum_{v_i \in \mathcal{V}} l(f_{\theta^*}(\tilde{v}_i(\theta_g), y_t)) + \mathcal{L}_U(\theta_g) + \beta \mathcal{L}_A(\theta^*, \theta_g) \quad s.t. \ \theta^* = \arg\min_{\theta} \mathcal{L}_f(\theta, \theta_g), \tag{10}$$

where β is the hyperparameter to control the contribution of prediction logic poisoning loss. θ_g denotes the parameters of the logic-poisoning trigger generator f_g. f_θ represents the surrogate GNN model, with θ as its parameters. The optimization algorithm for solving Eq.(10) is in Appendix F, and the overall training algorithm of Ba-Logic is in Appendix G.

5 Experiments

In this section, we conduct experiments to answer the following **R**esearch **Q**uestions:

- **RQ1**: Does Ba-Logic outperform the competitors under the clean-label setting?
- **RQ2**: Can Ba-Logic be generalized to more GNN downstream tasks and graphs?
- **RQ3**: Can Ba-Logic maintain high ASR against various defense strategies?
- **RQ4**: How effective are Ba-Logic's components for clean-label graph backdoor attacks?

5.1 Experimental Settings

Datasets We conduct experiments on **Cora** and **Pubmed** of Sen et al. (2008), **Flickr** Zeng et al. (2020), and **Arxiv** Hu et al. (2020) for node classification; **MUTAG**, **NCI1**, and **PROTEINS** of Morris et al. (2020) for graph classification; **Cora** of Sen et al. (2008), **CS** and **Physics** of Hu et al. (2020) for edge prediction. We also include heterophilous graphs with diverse scales, including **Squirrel** and **Chameleon** of Luan et al. (2022), **Penn** and **Genius** of Lim et al. (2021). More details of the datasets are in Appendix C.1.

Baselines We compare Ba-Logic with state-of-the-art graph backdoor attacks including **GTA** Xi et al. (2021), **EBA** Xu et al. (2021), **DPGBA** Zhang et al. (2024b), and **UGBA** Dai et al. (2023) under clean-label settings, denoted by **-C**. We also compare with the latest clean-label graph backdoor attacks, including **ERBA** Xu & Picek (2022) and **ECGBA** Fan & Dai (2024). We further extend comparison to **SCLBA** Dai & Sun (2025), **GCLBA** Meguro et al. (2024), **TRAP** Yang et al. (2022) for graph classification; and include **SNTBA** Dai & Sun (2024), **PSO-LB** and **LB** Zheng et al. (2023) for edge prediction. More details of the baselines are in Appendix C.2.

Evaluation In this paper, we focus on an inductive setting where attackers cannot access test samples during the graph poisoning. To reduce randomness, we conduct experiments on each target model 5 times and report the average results. The backdoor attacks are evaluated by ASR on the target nodes and CA on the clean nodes. More implementation details of Ba-Logic are in Appendix C.3.

5.2 Clean-Label Backdoor Performance

To answer **RQ1**, we compare Ba-Logic with the baselines across four datasets and three target GNNs. The surrogate model deployed for evaluation is a fixed 2-layer GCN. We report ASR | CA

Table 3: Average backdoor attack success rate and clean accuracy (ASR | CA (%)). Note that the surrogate model deployed in BA-LOGIC is fixed as a 2-layer GCN.

Dataset	Target Model	Vanilla Acc.	ERBA	ECGBA	EBA-C	GTA-C	UGBA-C	DPGBA-C	BA-LOGIC
Cora	GCN	83.78	18.22 | 80.77	34.77 | 79.48	29.13 | 74.17	32.45 | 80.45	68.32 | 79.97	59.55 | 79.88	**98.52 | 83.59**
	GAT	84.30	19.32 | 82.08	35.19 | 78.93	29.34 | 74.23	35.85 | 82.68	68.76 | 82.81	59.02 | 84.19	**97.12 | 83.76**
	GIN	84.26	19.17 | 79.85	34.56 | 79.92	29.30 | 74.46	35.49 | 79.63	67.75 | 83.04	60.03 | 81.56	**98.97 | 83.81**
Pubmed	GCN	86.38	22.18 | 85.58	37.46 | 85.86	31.89 | 85.60	38.84 | 86.17	71.24 | 85.31	64.19 | 85.41	**96.75 | 86.03**
	GAT	86.51	22.24 | 85.91	41.54 | 85.61	30.13 | 85.46	42.14 | 85.78	66.07 | 86.33	67.05 | 85.21	**94.88 | 85.13**
	GIN	86.51	15.46 | 85.57	43.14 | 83.63	30.99 | 85.44	42.34 | 86.35	68.69 | 85.81	66.17 | 86.22	**99.04 | 86.21**
Flickr	GCN	46.21	0.00 | 45.75	39.47 | 45.68	32.47 | 45.68	48.12 | 44.96	66.49 | 43.99	69.66 | 42.93	**99.98 | 46.05**
	GAT	46.07	0.00 | 47.51	41.03 | 47.65	31.93 | 47.65	47.87 | 47.64	68.78 | 47.02	70.39 | 46.31	**99.72 | 44.91**
	GIN	46.22	0.00 | 45.62	41.71 | 41.64	32.07 | 41.64	48.04 | 45.03	68.97 | 45.98	68.12 | 45.09	**100.0 | 46.14**
Arxiv	GCN	66.58	0.01 | 66.14	25.56 | 66.16	28.64 | 66.23	37.16 | 66.29	69.71 | 66.57	58.96 | 66.82	**98.04 | 65.82**
	GAT	66.02	0.02 | 64.09	26.03 | 64.46	28.09 | 64.41	36.45 | 65.20	71.65 | 65.10	59.13 | 65.25	**98.43 | 65.40**
	GIN	66.73	0.02 | 66.07	26.72 | 62.01	27.35 | 66.08	34.32 | 65.87	71.01 | 66.56	60.50 | 66.73	**97.62 | 66.83**

(%) of methods in Tab. 3, from which we observe: **(i)** Across all datasets and models, BA-LOGIC consistently achieves the highest ASR, typically close to 100%. It outperforms leading competitors such as UGBA-C and DPGBA-C, indicating that the clean-label setting is challenging for state-of-the-art methods, and BA-LOGIC poisons inner prediction logic of target models effectively for clean-label backdoor attacks. **(ii)** Arxiv poses challenges with its diverse classes and our fixed target class setting. Despite requiring generalization to larger unseen graph parts, BA-LOGIC maintains superior performance when the ASR of competitors drops, demonstrating its scalability. Experiments on larger graphs are in Appendix A.2. **(iii)** High ASR of BA-LOGIC towards different target GNNs proves its transferability in backdooring various GNNs via logic poisoning. More results of varying the surrogate and target models are in Appendix A.3. We further investigate how sampling strategies, where only a subset of nodes is involved during the aggregation, affect BA-LOGIC's performance in Appendix A.4 **(iv)** BA-LOGIC achieves comparable CA compared to vanilla GNN models, while other methods exhibit significantly larger CA drop. This indicates that our approach of poisoning the prediction logic hardly affects the prediction on clean nodes while achieving effective backdoor attacks. More experiments on the CA drop are provided in Appendix A.5.

5.3 GENERALIZATION TO MORE TASKS AND GRAPHS

Considering that node classification, graph classification, edge prediction can all be formed into graph classification task, A natural question is how our BA-LOGIC can be generalized to graph classification and edge prediction. Therefore, to answer **RQ2**, we extend BA-LOGIC from node classification to graph classification and edge prediction. Details of the extensions are provided in Appendix A.1. Tab. 4 reports results for graph classification and for edge prediction. From the results, we observe that BA-LOGIC achieves competitive or superior performance in backdooring both graph classification and edge prediction tasks without degrading clean accuracy, highlighting the effectiveness of the extended BA-LOGIC.

Table 4: Evaluation (ASR | CA (%)) of BA-LOGIC on more tasks.

Graph Classification					**Edge Prediction**				
Dataset	**SCLBA**	**GCLBA**	**TRAP**	**BA-LOGIC**	**Dataset**	**SNTBA**	**PSO-LB**	**LB**	**BA-LOGIC**
MUTAG	88.51|62.77	19.27|62.81	71.89|61.44	92.17|61.32	Cora	91.32|80.43	61.35|79.45	68.06|76.17	99.01|79.59
NCI1	94.01|61.43	61.35|60.97	68.06|61.51	96.19|62.08	CS	89.62|81.95	67.14|76.13	57.67|78.49	95.13|79.65
PROTEINS	67.59|71.25	67.14|71.33	57.67|71.49	89.67|71.65	Physics	48.32|62.77	39.27|64.09	61.89|63.44	93.81|63.02

We further assess BA-LOGIC on diverse heterophilous graphs for node classification. Tab. 5 reports the results when targeting the heterophily-specific GNN models ACMGCN Luan et al. (2022) and LINKX Lim et al. (2021), along with the results when targeting GCN. Results in Tab. 5 indicate that graph characteristics such as heterophily mainly affect the CA of GNNs instead of the ASR of BA-LOGIC, which adopts logic poisoning to ensure high ASR across various graphs and backbones. More comparison with base-

Table 5: Results (ASR | CA (%)) of BA-LOGIC in backdooring heterophilous graphs.

Datasets	**GCN**	**ACMGCN**	**LINKX**
Squirrel	99.07 | 44.76	98.14 | 65.37	98.79 | 71.90
Chameleon	99.03 | 51.18	98.53 | 68.58	98.43 | 81.22
Penn	96.34 | 65.47	96.71 | 72.52	95.32 | 72.32
Genius	98.17 | 79.42	97.92 | 88.72	93.71 | 89.14

lines transferred from other domains is in Appendix A.6. More analysis on the generalizability of BA-LOGIC under challenging label and feature settings is in Appendix K.

5.4 ATTACKS ON DEFENDING STRATEGIES

To answer **RQ3**, we evaluate BA-LOGIC and competitors against representative defense methods, including GCN-Prune Dai et al. (2023), RobustGCN Zhu et al. (2019), GNNGuard Zhang & Zitnik (2020), and RIGBD Zhang et al. (2025). We record experiments conducted on two datasets in Tab. 6. From the table, we observe: **(i)** BA-LOGIC can effectively attack the robust GNN models. Compared with competitors, BA-LOGIC enhances ASR by 30%, showing the superiority of BA-LOGIC in conducting backdoor attacks against defense methods by logic poisoning. **(ii)** Although RIGBD is highly effective in defending against various backdoor attacks, it fails to defend against BA-LOGIC that generates logic poisoning triggers. RIGBD defends by identifying the poisoned target nodes and random edge dropping. Its failure arises from the inability to alleviate the logic poisoning caused by BA-LOGIC during the training of target GNNs, confirming our method's effectiveness. More results of attacking defenses is provided in Appendix A.7 and Appendix I.

Table 6: Comparisons of ASR(%) against defense models.

Datasets	Defense	ECGBA	DPGBA-C	UGBA-C	BA-LOGIC
Flickr	GCN-Prune	15.02	35.44	54.49	**99.24**
	RobustGCN	11.25	22.26	58.81	**99.02**
	GNNGuard	0.01	53.41	33.14	**99.36**
	RIGBD	0.01	0.07	0.33	**94.86**
Arxiv	GCN-Prune	13.57	17.43	62.31	**96.75**
	RobustGCN	14.24	29.65	44.46	**97.03**
	GNNGuard	0.51	43.77	40.08	**95.37**
	RIGBD	0.01	0.01	0.19	**93.23**

5.5 ABLATION STUDIES

To answer **RQ4**, we conduct ablation studies to explore the effectiveness of the poisoned node selector and the logic-poisoning trigger generator. To demonstrate the effectiveness of the poisoned node selector, we randomly select poisoned nodes from the training graph and obtain a variant named BA-LOGIC\S. To show the benefits of the logic poisoning trigger generator, we remove the inner logic loss in Eq.(7). In such a case, the BA-LOGIC degrades to a simplified variant named BA-LOGIC\T. To verify the effect of module collaboration, we implement BA-LOGIC by removing both modules, named as BA-LOGIC\ST. The ASR with standard deviations on Pubmed and Arxiv are shown in Fig. 4, from which we observe: **(i)** Compare to BA-LOGIC\S, BA-LOGIC achieves better attack performance on various datasets. The standard variance of ASR of BA-LOGIC is significantly lower than that of BA-LOGIC\S. It indicates that our selector identifies poisoned nodes that are influential to logic poisoning backdoor attacks. **(ii)** BA-LOGIC outperforms BA-LOGIC\T and BA-LOGIC\ST by a large margin. It highlights the proposed logic poisoning loss guides the trigger generator to produce triggers capable of poisoning the inner logic of the target model for various test nodes. More analysis to evaluate the contribution of each module is provided in Appendix A.8.

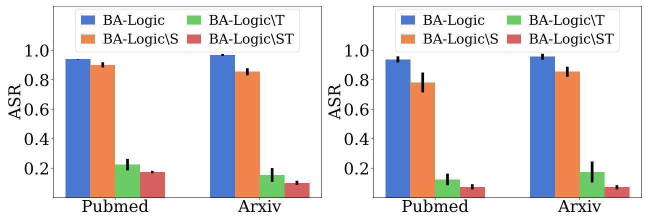

(a) GCN (b) GIN

Figure 4: Ablation studies of BA-LOGIC.

6 CONCLUSION AND FUTURE WORKS

In this paper, we investigate the limitations of existing graph backdoor attacks under a clean-label setting. To overcome these limitations, we formalize the problem of clean-label graph backdoor attacks through poisoning the inner prediction logic of GNNs. Our methodology originates from the preliminary analysis of learning behaviors in backdoored GNNs, leading to a theoretically grounded learning objective formulated as bi-level optimization for effective model poisoning. Extensive experiments on real-world datasets with diverse graph learning tasks demonstrate that our approach successfully induces backdoor behaviors in various GNN architectures under clean-label constraints, and BA-LOGIC remains resilient against existing backdoor defense methods. Fundamentally, our results primarily support our argument on poisoning the inner prediction logic of GNNs for effective clean-label graph backdoor attacks. Several promising directions emerge for future research, including extending research scope to other tasks like recommendation systems, and developing defense strategies against logic poisoning through the inverse application of our methodology.

Ethics statement

In this work, we investigate potential security vulnerabilities in Graph Neural Networks (GNNs) by developing a inner prediction logic poisoning clean-label graph backdoor attack without modifying present labels. We recognize that the study of logic poisoning backdoor attacks may raise concerns regarding potential risks. However, our primary goal is to advance the understanding of such vulnerabilities to foster the development of more robust and trustworthy GNN models. We believe this work will encourage further research into understanding clean-label graph backdoor attacks and contribute to improving the safety and reliability of graph learning methods.

Reproducibility statement

In this work, we proposed a novel approach to poison the inner prediction logic of Graph Neural Networks (GNNs) for effectively conducting clean-label graph backdoor attacks. To ensure the reproducibility of our work, we have provided comprehensive details throughout the paper and supplementary materials. The methodology of our proposed Ba-Logic framework is described in detail in Section 4. Furthermore, Appendix C contains a complete description of the implementation, including the public datasets used, adaptations of baseline methods, and the specific training parameters for Ba-Logic. The source code of Ba-Logic is available in an anonymous repository, with the link provided at the end of the Abstract. Additionally, for our theoretical analysis, Appendix H provides a complete proof of Theorem 1, explicitly stating all underlying assumptions.

References

Eiman Alothali, Nazar Zaki, Elfadil A Mohamed, and Hany Alashwal. Detecting social bots on twitter: a literature review. In *2018 International conference on innovations in information technology (IIT)*, pp. 175–180. IEEE, 2018.

Federico Baldassarre and Hossein Azizpour. Explainability techniques for graph convolutional networks. In *International Conference on Machine Learning (ICML) Workshops, 2019 Workshop on Learning and Reasoning with Graph-Structured Representations*, 2019.

Pietro Bongini, Monica Bianchini, and Franco Scarselli. Molecular generative graph neural networks for drug discovery. *Neurocomputing*, 450:242–252, 2021.

Jie Chen, Tengfei Ma, and Cao Xiao. Fastgcn: Fast learning with graph convolu-tional networks via importance sampling. In *International Conference on Learning Representations*. International Conference on Learning Representations, ICLR, 2018.

Ming Chen, Zhewei Wei, Zengfeng Huang, Bolin Ding, and Yaliang Li. Simple and deep graph convolutional networks. In *International conference on machine learning*, pp. 1725–1735. PMLR, 2020.

Yang Chen and Bin Zhou. Agsoa: Graph neural network targeted attack based on average gradient and structure optimization. *arXiv preprint arXiv:2406.13228*, 2024.

Dawei Cheng, Fangzhou Yang, Sheng Xiang, and Jin Liu. Financial time series forecasting with multi-modality graph neural network. *Pattern Recognition*, 121:108218, 2022.

Enyan Dai and Suhang Wang. Say no to the discrimination: Learning fair graph neural networks with limited sensitive attribute information. In *WSDM*, pp. 680–688, 2021a.

Enyan Dai and Suhang Wang. Towards self-explainable graph neural network. In *CIKM*, pp. 302–311, 2021b.

Enyan Dai, Wei Jin, Hui Liu, and Suhang Wang. Towards robust graph neural networks for noisy graphs with sparse labels. In *WSDM*, pp. 181–191, 2022a.

Enyan Dai, Shijie Zhou, Zhimeng Guo, and Suhang Wang. Label-wise graph convolutional network for heterophilic graphs. In *Learning on Graphs Conference*, pp. 26–1. PMLR, 2022b.

Enyan Dai, Minhua Lin, Xiang Zhang, and Suhang Wang. Unnoticeable backdoor attacks on graph neural networks. In *Proceedings of the ACM Web Conference 2023*, pp. 2263–2273, 2023.

Enyan Dai, Tianxiang Zhao, Huaisheng Zhu, Junjie Xu, Zhimeng Guo, Hui Liu, Jiliang Tang, and Suhang Wang. A comprehensive survey on trustworthy graph neural networks: Privacy, robustness, fairness, and explainability. *Machine Intelligence Research*, pp. 1–51, 2024.

Jiazhu Dai and Haoyu Sun. A backdoor attack against link prediction tasks with graph neural networks. *arXiv preprint arXiv:2401.02663*, 2024.

Jiazhu Dai and Haoyu Sun. A semantic and clean-label backdoor attack against graph convolutional networks. *arXiv preprint arXiv:2503.14922*, 2025.

Yian Deng and Tingting Mu. Understanding and improving ensemble adversarial defense. *Advances in Neural Information Processing Systems*, 36:58075–58087, 2023.

Abhijeet Dhali and Renata Dividino. The power of many: Investigating defense mechanisms for resilient graph neural networks. In *2024 IEEE International Conference on Big Data (BigData)*, pp. 3572–3578. IEEE, 2024.

Paul Erdos, Alfréd Rényi, et al. On the evolution of random graphs. *Publ. math. inst. hung. acad. sci*, 5(1):17–60, 1960.

Xuanhao Fan and Enyan Dai. Effective clean-label backdoor attacks on graph neural networks. In *Proceedings of the 33rd ACM International Conference on Information and Knowledge Management*, pp. 3752–3756, 2024.

Johannes Gasteiger, Aleksandar Bojchevski, and Stephan Günnemann. Combining neural networks with personalized pagerank for classification on graphs. In *International Conference on Learning Representations*, 2019.

Justin Gilmer, Samuel S Schoenholz, Patrick F Riley, Oriol Vinyals, and George E Dahl. Message passing neural networks. In *Machine learning meets quantum physics*, pp. 199–214. Springer, 2020.

Wei Guo, Benedetta Tondi, and Mauro Barni. A temporal chrominance trigger for clean-label backdoor attack against anti-spoof rebroadcast detection. *IEEE Transactions on Dependable and Secure Computing*, 20(6):4752–4762, 2023.

Will Hamilton, Zhitao Ying, and Jure Leskovec. Inductive representation learning on large graphs. *Advances in neural information processing systems*, 30, 2017.

Weihua Hu, Matthias Fey, Marinka Zitnik, Yuxiao Dong, Hongyu Ren, Bowen Liu, Michele Catasta, and Jure Leskovec. Open graph benchmark: Datasets for machine learning on graphs. *Advances in neural information processing systems*, 33:22118–22133, 2020.

Qiang Huang, Makoto Yamada, Yuan Tian, Dinesh Singh, and Yi Chang. Graphlime: Local interpretable model explanations for graph neural networks. *IEEE Transactions on Knowledge and Data Engineering*, 35(7):6968–6972, 2022.

Itay Hubara, Matthieu Courbariaux, Daniel Soudry, Ran El-Yaniv, and Yoshua Bengio. Binarized neural networks. *Advances in neural information processing systems*, 29, 2016.

James Kennedy and Russell Eberhart. Particle swarm optimization. In *Proceedings of ICNN'95-international conference on neural networks*, volume 4, pp. 1942–1948. ieee, 1995.

Thomas N. Kipf and Max Welling. Semi-supervised classification with graph convolutional networks. In *International Conference on Learning Representations*, 2017. URL `https://openreview.net/forum?id=SJU4ayYgl`.

Derek Lim, Felix Hohne, Xiuyu Li, Sijia Linda Huang, Vaishnavi Gupta, Omkar Bhalerao, and Ser Nam Lim. Large scale learning on non-homophilous graphs: New benchmarks and strong simple methods. *Advances in neural information processing systems*, 34:20887–20902, 2021.

Sitao Luan, Chenqing Hua, Qincheng Lu, Jiaqi Zhu, Mingde Zhao, Shuyuan Zhang, Xiao-Wen Chang, and Doina Precup. Revisiting heterophily for graph neural networks. *Advances in neural information processing systems*, 35:1362–1375, 2022.

Dongsheng Luo, Wei Cheng, Dongkuan Xu, Wenchao Yu, Bo Zong, Haifeng Chen, and Xiang Zhang. Parameterized explainer for graph neural network. *Advances in neural information processing systems*, 33:19620–19631, 2020.

Yuankai Luo, Lei Shi, and Xiao-Ming Wu. Classic gnns are strong baselines: Reassessing gnns for node classification. *Advances in Neural Information Processing Systems*, 37:97650–97669, 2024.

Ryo Meguro, Hiroya Kato, Shintaro Narisada, Seira Hidano, Kazuhide Fukushima, Takuo Suganuma, and Masahiro Hiji. Gradient-based clean label backdoor attack to graph neural networks. In *ICISSP*, pp. 510–521, 2024.

Christopher Morris, Nils M. Kriege, Franka Bause, Kristian Kersting, Petra Mutzel, and Marion Neumann. Tudataset: A collection of benchmark datasets for learning with graphs. In *ICML 2020 Workshop on Graph Representation Learning and Beyond (GRL+ 2020)*, 2020. URL `www.graphlearning.io`.

Xuelian Ni, Fei Xiong, Yu Zheng, and Liang Wang. Graph contrastive learning with kernel dependence maximization for social recommendation. In *Proceedings of the ACM Web Conference 2024*, pp. 481–492, 2024.

Phillip E Pope, Soheil Kolouri, Mohammad Rostami, Charles E Martin, and Heiko Hoffmann. Explainability methods for graph convolutional neural networks. In *Proceedings of the IEEE/CVF conference on computer vision and pattern recognition*, pp. 10772–10781, 2019.

Thomas Schnake, Oliver Eberle, Jonas Lederer, Shinichi Nakajima, Kristof T Schütt, Klaus-Robert Müller, and Grégoire Montavon. Higher-order explanations of graph neural networks via relevant walks. *IEEE transactions on pattern analysis and machine intelligence*, 44(11):7581–7596, 2021.

Ramprasaath R Selvaraju, Michael Cogswell, Abhishek Das, Ramakrishna Vedantam, Devi Parikh, and Dhruv Batra. Grad-cam: Visual explanations from deep networks via gradient-based localization. In *Proceedings of the IEEE international conference on computer vision*, pp. 618–626, 2017.

Prithviraj Sen, Galileo Namata, Mustafa Bilgic, Lise Getoor, Brian Galligher, and Tina Eliassi-Rad. Collective classification in network data. *AI magazine*, 29(3):93–93, 2008.

Jiabin Tang, Lianghao Xia, and Chao Huang. Explainable spatio-temporal graph neural networks. In *Proceedings of the 32nd ACM International Conference on Information and Knowledge Management*, pp. 2432–2441, 2023.

Petar Veličković, Guillem Cucurull, Arantxa Casanova, Adriana Romero, Pietro Liò, and Yoshua Bengio. Graph attention networks. In *International Conference on Learning Representations*, 2018. URL `https://openreview.net/forum?id=rJXMpikCZ`.

Huiwei Wang, Tianhua Liu, Ziyu Sheng, and Huaqing Li. Explanatory subgraph attacks against graph neural networks. *Neural Networks*, 172:106097, 2024a.

Jie Wang, Zheng Yan, Jiahe Lan, Elisa Bertino, and Witold Pedrycz. Trustguard: Gnn-based robust and explainable trust evaluation with dynamicity support. *IEEE Transactions on Dependable and Secure Computing*, 2024b.

Kaiyang Wang, Huaxin Deng, Yijia Xu, Zhonglin Liu, and Yong Fang. Multi-target label backdoor attacks on graph neural networks. *Pattern Recognition*, 152:110449, 2024c.

Xiaoqi Wang and Han Wei Shen. Gnnboundary: Towards explaining graph neural networks through the lens of decision boundaries. In *The Twelfth International Conference on Learning Representations*, 2024.

Zhenzhong Wang, Lulu Cao, Wanyu Lin, Min Jiang, and Kay Chen Tan. Robust graph meta-learning via manifold calibration with proxy subgraphs. In *Proceedings of the AAAI Conference on Artificial Intelligence*, volume 37, pp. 15224–15232, 2023.

Felix Wu, Amauri Souza, Tianyi Zhang, Christopher Fifty, Tao Yu, and Kilian Weinberger. Simplifying graph convolutional networks. In *International conference on machine learning*, pp. 6861–6871. PMLR, 2019.

Zhaohan Xi, Ren Pang, Shouling Ji, and Ting Wang. Graph backdoor. In *USENIX Security*, pp. 1523–1540, 2021.

Hui Xia, Xiangwei Zhao, Rui Zhang, Shuo Xu, and Luming Wang. Clean-label graph backdoor attack in the node classification task. In *Proceedings of the AAAI Conference on Artificial Intelligence*, volume 39, pp. 21626–21634, 2025.

Xiaogang Xing, Ming Xu, Yujing Bai, and Dongdong Yang. A clean-label graph backdoor attack method in node classification task. *Knowledge-Based Systems*, 304:112433, 2024.

Jing Xu and Stjepan Picek. Poster: clean-label backdoor attack on graph neural networks. In *Proceedings of the 2022 ACM SIGSAC Conference on Computer and Communications Security*, pp. 3491–3493, 2022.

Jing Xu, Minhui Xue, and Stjepan Picek. Explainability-based backdoor attacks against graph neural networks. In *Proceedings of the 3rd ACM workshop on wireless security and machine learning*, pp. 31–36, 2021.

Keyulu Xu, Weihua Hu, Jure Leskovec, and Stefanie Jegelka. How powerful are graph neural networks? In *International Conference on Learning Representations*, 2019. URL `https://openreview.net/forum?id=ryGs6iA5Km`.

Shuiqiao Yang, Bao Gia Doan, Paul Montague, Olivier De Vel, Tamas Abraham, Seyit Camtepe, Damith C Ranasinghe, and Salil S Kanhere. Transferable graph backdoor attack. In *Proceedings of the 25th international symposium on research in attacks, intrusions and defenses*, pp. 321–332, 2022.

Jun Yin, Chaozhuo Li, Hao Yan, Jianxun Lian, and Senzhang Wang. Train once and explain everywhere: Pre-training interpretable graph neural networks. *Advances in Neural Information Processing Systems*, 36:35277–35299, 2023.

Zhitao Ying, Dylan Bourgeois, Jiaxuan You, Marinka Zitnik, and Jure Leskovec. Gnnexplainer: Generating explanations for graph neural networks. *Advances in neural information processing systems*, 32, 2019.

Hanqing Zeng, Hongkuan Zhou, Ajitesh Srivastava, Rajgopal Kannan, and Viktor Prasanna. Graphsaint: Graph sampling based inductive learning method. In *International Conference on Learning Representations*, 2020. URL `https://openreview.net/forum?id=BJe8pkHFwS`.

Chuxu Zhang, Dongjin Song, Chao Huang, Ananthram Swami, and Nitesh V Chawla. Heterogeneous graph neural network. In *Proceedings of the 25th ACM SIGKDD international conference on knowledge discovery & data mining*, pp. 793–803, 2019.

He Zhang, Bang Wu, Xingliang Yuan, Shirui Pan, Hanghang Tong, and Jian Pei. Trustworthy graph neural networks: Aspects, methods, and trends. *Proceedings of the IEEE*, 112(2):97–139, 2024a.

Xiang Zhang and Marinka Zitnik. Gnnguard: Defending graph neural networks against adversarial attacks. *Advances in neural information processing systems*, 33:9263–9275, 2020.

Zaixi Zhang, Jinyuan Jia, Binghui Wang, and Neil Zhenqiang Gong. Backdoor attacks to graph neural networks. In *Proceedings of the 26th ACM Symposium on Access Control Models and Technologies*, pp. 15–26, 2021.

Zhiwei Zhang, Minhua Lin, Enyan Dai, and Suhang Wang. Rethinking graph backdoor attacks: A distribution-preserving perspective. In *Proceedings of the 30th ACM SIGKDD Conference on Knowledge Discovery and Data Mining*, pp. 4386–4397, 2024b.

Zhiwei Zhang, Minhua Lin, Junjie Xu, Zongyu Wu, Enyan Dai, and Suhang Wang. Robustness inspired graph backdoor defense. In *The Thirteenth International Conference on Learning Representations*, 2025.

Shihao Zhao, Xingjun Ma, Xiang Zheng, James Bailey, Jingjing Chen, and Yu-Gang Jiang. Clean-label backdoor attacks on video recognition models. In *Proceedings of the IEEE/CVF conference on computer vision and pattern recognition*, pp. 14443–14452, 2020.

Haibin Zheng, Haiyang Xiong, Haonan Ma, Guohan Huang, and Jinyin Chen. Link-backdoor: Backdoor attack on link prediction via node injection. *IEEE Transactions on Computational Social Systems*, 11(2):1816–1831, 2023.

Bolei Zhou, Aditya Khosla, Agata Lapedriza, Aude Oliva, and Antonio Torralba. Learning deep features for discriminative localization. In *Proceedings of the IEEE conference on computer vision and pattern recognition*, pp. 2921–2929, 2016.

Dingyuan Zhu, Ziwei Zhang, Peng Cui, and Wenwu Zhu. Robust graph convolutional networks against adversarial attacks. In *Proceedings of the 25th ACM SIGKDD international conference on knowledge discovery & data mining*, pp. 1399–1407, 2019.

Jiong Zhu, Yujun Yan, Lingxiao Zhao, Mark Heimann, Leman Akoglu, and Danai Koutra. Beyond homophily in graph neural networks: Current limitations and effective designs. *Advances in neural information processing systems*, 33:7793–7804, 2020.

APPENDIX CONTENTS

A Additional Experiments

A.1 Additional Discussion on Extending Method

In the main text, we initially design Ba-Logic for node classification and subsequently extend it to graph classification and edge prediction for evaluation. This extension is grounded in the fact that these graph learning tasks are all built upon the common message-passing mechanism of GNNs Gilmer et al. (2020), where the core objective is to learn representations by aggregating information from neighbors, which can be nodes, edges, and graphs. While the specific readout functions differ across the tasks, such as node-level output for node classification, graph-level pooling for graph classification, and pairwise node scoring for edge prediction, the underlying mechanism for generating embeddings is shared.

We presented the results in Tab. 4, demonstrating the consistent effectiveness of Ba-Logic on conducting clean-label graph backdoor attacks on diverse tasks. Below, we detail the extensions of Ba-Logic for graph classification and edge prediction, respectively.

A.1.1 Extend Ba-Logic to Graph Classification

We first discuss how to extend our Ba-Logic to graph classification. To backdoor graph classification, we select the training graph G_i from the target class y_t to establish a poisoned graph set $\mathcal{G}_P$, and replace its nodes with trigger g_i to poison the inner logic of target GNN models. For node $v_j \in G_i$ and target class y_t, importance score originates from Eq.(6) can be computed by:

$$S(y_i^t, v_j) = ||\frac{\partial \tilde{y}_i^c}{\partial \mathbf{x}_j}||_2 \tag{11}$$

And the logic poisoning loss originates from Eq.(7) can be computed by:

$$\mathcal{L}_A = \sum_{v_i \in G_i} \max(0, T - (\sum_{v_g \in g_i} S(y_i^t, v_g) - \sum_{v_c \in G_i \setminus g_i} S(y_i^t, v_c))) \tag{12}$$

Moreover, the adopted lower-level optimization originates from Eq.(15) aims to train θ on clean graphs $\mathcal{G}_L \setminus \mathcal{G}_P$ and poisoned graph set $\mathcal{G}_P$. The upper-level optimization, originating from Eq.(16), aims to optimize θ_g to minimize the loss for predicting $\mathcal{G}_P$ as y_t. To keep the trigger unnoticeable when against defense methods, constraint in Eq.(8) on θ_g should be kept.

With the adaptation stated above, we extend our method to select graph classification as a downstream task. In practice, we select a 2-layer GCN as the surrogate model, and report the average performance of three different target models, i.e., GCN, GIN, and GAT. Moreover, we add a global pooling layer to both the surrogate and target models and update the classifier for graph classification.

A.1.2 Extend Ba-Logic to Edge Prediction

Noting that edge prediction is another widely adopted downstream task for GNN models besides node classification and graph classification, we further discuss how to extend our Ba-Logic to backdoor GNN models that select edge prediction as the downstream task.

We consider the extension from a node-oriented perspective, in which the attacker attaches a trigger $g_{u,v}$ to node u to make the model predict an edge (u, v) based on the trigger. To achieve this, we maximize the influence of trigger nodes relative to clean neighbors. For node v_j and edge (u, v), the importance score of v_j in predicting the edge is originated from Eq.(6), which can be formulated by:

$$S((u, v), v_j) = ||\frac{\partial \tilde{y}_{(u,v)}}{\partial \mathbf{x}_j}||_2, \tag{13}$$

where $\tilde{y}_{(u,v)}$ is the edge prediction given by the target model.

To backdoor edge prediction, we adopt logic poisoning loss, originating from Eq.(7), to maximize the influence of trigger nodes relative to clean neighbors. After attaching the trigger, the logic poisoning loss should be:

$$\mathcal{L}_A = \sum_{(u,v) \in \mathcal{E}} \max(0, T - (\sum_{v_g \in g_{u,v}} S((u, v), v_g) - \sum_{v_c \in \mathcal{N}_u} S((u, v), v_c))), \tag{14}$$

where $\mathcal{E}$ is the edge set, $\mathcal{N}_u$ are clean neighbors.

Moreover, the adopted lower-level optimization originates from Eq.(15) aims to train θ on clean edges ($\mathcal{E}_L \setminus \mathcal{E}_P$) and poisoned edges ($\mathcal{E}_P$). The upper-level optimization, originating from Eq.(16), aims to optimize the trigger generator θ_g for minimizing the prediction loss on $\mathcal{E}_P$. To keep the trigger unnoticeable when against defense methods, the constraint in Eq.(8) on θ_g should be kept.

With the adaptation stated above, we extend our method to select edge prediction as a downstream task. In practice, we select a 2-layer GCN as the surrogate model, and report the average performance of three different target models, i.e., GCN, GIN, and GAT.

A.2 Additional Results of Attack Performance on Industry-Scale Graph

In the main text of our work, we have included multiple graph datasets with diverse characteristics for evaluation. To further demonstrate the scalability of Ba-Logic, we evaluate our method on OGBN-Products Hu et al. (2020), an industry-scale node classification dataset with 2.4 million nodes. Specifically, we select a 5-layer GCN and GraphSAGE as the surrogate model, and report the ASR|CA(%) of selecting GCN as the target model with the same layers. Due to the large size of OGBN-Products, which prevents full-batch training on GPU memory, we enabled mini-batch training with a large batch size following Luo et al. (2024). It is feasible in practice, as our method is not strongly dependent on graph structure and only requires approximate linear complexity. We also record the training time and GPU memory information during Ba-Logic conducting backdoor attacks. The results are recorded in Tab. 7, from which we have the following key findings:

Table 7: Training statistics and performance of Ba-Logic on **OGBN-Products**.

Surrogate Model	**Training Time (s)**	**GPU Memory Peak (GB)**	**ASR|CA (%)**
GCN	1678.05	23.52	87.07 | 78.51
GraphSAGE	1531.39	22.36	83.69 | 80.27

- The scalability of our method is demonstrated with feasible resource usage on a large graph with 2.4 million nodes, indicating that our Ba-Logic remains practical at an industrial scale.
- Training time is acceptable given the performance, consistent with the approximately linear complexity with respect to graph size per optimization iteration as shown in Appendix B.

A.3 Additional Results of Varying Surrogate and Target Models

In the main text of our work, we deliberately fixed a normal 2-layer GCN as the surrogate model when evaluating with diverse target models, such as GIN, GAT, etc. Here, we further test triggers crafted on one surrogate model against different target models to highlight the transferability of our method. Specifically, we conduct additional experiments on **Cora** and **Arxiv** by varying both the surrogate and target models across all six backbones implemented in both the main text and the Appendix A.4. Tab. 8 and 9 present the results, from which we have the following key findings:

Table 8: Results (ASR|CA(%)) of varying surrogate and target models on **Cora**.

Target \ **Surrogate**	**GCN**	**GAT**	**GIN**	**GraphSAGE**	**GraphSAINT**	**FastGCN**
GCN	98.52 | 83.59	98.49 | 82.97	98.31 | 81.26	98.45 | 81.59	97.43 | 80.69	94.23 | 81.43
GAT	97.12 | 83.76	97.17 | 82.18	98.75 | 83.66	99.02 | 82.25	96.05 | 82.29	93.24 | 81.56
GIN	98.97 | 83.81	97.48 | 83.27	97.12 | 82.58	97.34 | 81.04	94.13 | 83.37	93.21 | 80.08
GraphSAGE	98.15 | 83.35	98.15 | 82.66	98.02 | 81.43	98.20 | 81.26	93.08 | 81.24	95.21 | 79.14
GraphSAINT	95.13 | 80.57	94.39 | 81.21	97.63 | 80.59	97.85 | 80.07	95.41 | 82.48	91.19 | 79.34
FastGCN	90.25 | 82.91	91.88 | 83.18	97.85 | 81.97	97.92 | 83.16	95.24 | 80.01	92.25 | 80.56

Table 9: Results (ASR|CA(%)) of varying surrogate and target models on **Arxiv**.

Target \ Surrogate	GCN	GAT	GIN	GraphSAGE	GraphSAINT	FastGCN
GCN	98.04 | 65.82	98.51 | 64.35	98.18 | 66.02	98.45 | 66.71	95.21 | 64.62	93.45 | 64.13
GAT	98.43 | 65.40	98.97 | 62.24	98.75 | 65.42	97.06 | 65.38	95.45 | 63.58	93.48 | 65.09
GIN	97.62 | 66.83	97.20 | 64.35	96.12 | 66.15	97.15 | 65.17	94.25 | 64.15	93.07 | 66.35
GraphSAGE	98.07 | 64.95	98.05 | 64.13	96.16 | 64.07	95.12 | 61.34	94.15 | 63.65	93.42 | 65.51
GraphSAINT	91.31 | 61.42	97.75 | 61.25	97.15 | 61.32	94.85 | 59.66	94.47 | 60.22	92.38 | 62.12
FastGCN	89.95 | 59.71	97.88 | 60.21	97.85 | 60.13	97.92 | 59.18	94.82 | 58.71	94.25 | 60.11

- Despite differences between surrogate and target models, our attack maintains high effectiveness, demonstrating strong transferability rooted in poisoning the shared message-passing mechanism for most GNNs.
- Sampling-based targets like GraphSAINT and FastGCN are slightly more robust to backdoors. We attribute this to their stochastic sampling of a subset of nodes which dilutes the trigger impact.

A.4 Additional Results of Attack Performance towards Sampling-Based GNNs

We evaluate BA-LOGIC with different graph sampling methods involved to explore the effectiveness of poisoning the logic of sampling-based GNNs. We expand our experiments by incorporating three widely adopted sampling-based GNNs: GraphSAGE Hamilton et al. (2017), GraphSAINT Zeng et al. (2020), and FastGCN Chen et al. (2018). Specifically, we have implemented GraphSAGE with two different graph pooling strategies, denoted as SAGE-max, SAGE-min, respectively. And we also implemented GraphSAINT with three different samplers, node, edge, and walk, denoted as SAINT-N, SAINT-E, and SAINT-W, respectively. To mitigate the randomness induced by sampling, we repeat each experiment 5 times and present the average results as shown in Fig. 5, from which we observe:

- Sampling methods can weaken BA-LOGIC slightly, as BA-LOGIC poisons the inner logic of the model by involving poison nodes attached to triggers in training.
- The impact is more significant when a large graph reduces the probability of sampling poison nodes. Specifically, ASR is most affected for layer-wise sampling (FastGCN) backbone, as it samples a fixed number of nodes in each layer; Moreover, ASR of node-wise sampling (GraphSAGE) and subgraph-wise sampling (GraphSAINT) backbones are not greatly affected, as the samplers will significantly increase the probability of sampling poison nodes.
- Among the three GraphSAINT samplers, BA-LOGIC achieves the highest ASR when facing SAINT-W. This is because SAINT-W can sample the complete trigger through random walks, amplifying the impact of logic poison.

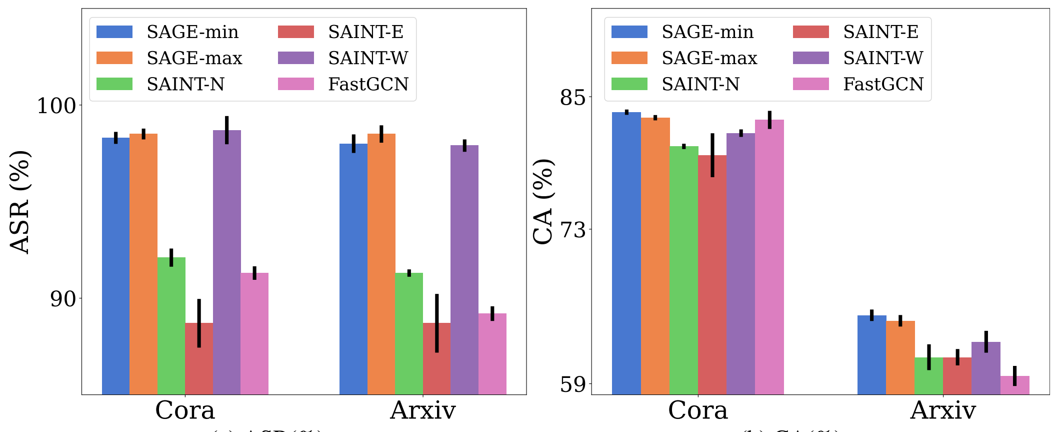

(a) ASR(%) (b) CA(%)

Figure 5: Performance of BA-LOGIC on sampling-based GNNs.

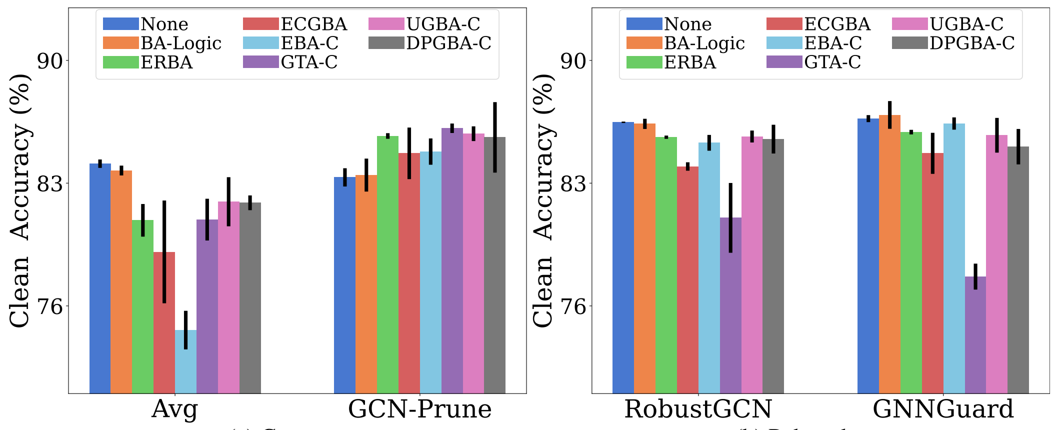

(a) Cora (b) Pubmed

Figure 6: Clean Accuracy of backdoored models.

A.5 Additional Results of Clean Accuracy Drop Analysis

In the main text, Table 3 shows that some existing methods may cause a drop in the model's clean accuracy during inference under certain conditions. This is inconsistent with the desired behavior of a backdoor attack, where only nodes containing the trigger should be misclassified as the target class, while predictions on clean nodes should remain unaffected to preserve clean accuracy. We illustrate the average clean accuracy and standard deviation of five runs of different backbones after being backdoored in Fig. 6. It should be noted that **Avg** represents the average results on GCN, GAT, and GIN, which are three target models we use in Tab. 3. From the figure, we can observe that:

- Nearly all methods show a decrease in clean accuracy, indicating that their backdoor attack process damages the normal behavior of the model, thereby weakening its practicality.
- Combined with the results of Tab. 3, certain baselines (e.g., EBA-C and ECGBA) severely degrade the clean accuracy of target models, which violates the backdoor attack's objective to maintain the classification accuracy of the model for clean test nodes.
- The degradation of clean accuracy caused by various methods is generally alleviated on the stronger defense models, RobustGCN and GNNGuard, which indicates the robustness of our selected defense methods and highlights the effectiveness of BA-LOGIC in conducting backdoor attacks.

A.6 Additional Comparison with Cross-Domain Baselines

In the main text of our work, we mainly focus on evaluating backdoor attacks in the graph domain. However, we found that the clean-label setting presents a shared challenge for both image and graph domains. And the representative works from the image domain solve unique challenges and make significant contributions in their respective fields. Specifically, we adopt the following backdoor methods from the image domain to the graph domain:

- **OPS-GFS** Guo et al. (2023): OPS-GFS presents a clean-label video backdoor attack, designing a temporal chrominance trigger to achieve imperceptible yet effective poisoning. This work proposes a temporal chrominance-based trigger, leveraging the peculiarities of the human visual system to reduce trigger visibility. To achieve effective poisoning in clean-label setting, the method utilizes an Outlier Poisoning Strategy (OPS). OPS selects poisoned video samples that the surrogate video model cannot classify. The attack is further enhanced by Ground-truth Feature Suppression (GFS), which suppresses the features of outlier samples.
- **UAT** Zhao et al. (2020): UAT proposes a clean-label video backdoor attack, employing a universal adversarial trigger to overcome high-dimensional input and unique clean-label challenges in video recognition. The method employs a Universal Adversarial Trigger (UAT), whose pattern is generated by minimizing the cross-entropy loss towards the target class across video samples from non-target classes. To enhance the trigger, the attack applies adversarial perturbation to videos

in the target class before injecting UAT. UAT coordinates two types of perturbation, uniform and targeted adversarial perturbation, to weaken original features.

To adapt OPS-GFS to the graph domain, we make the following efforts:

- To adapt OPS strategy, we select the misclassified training graphs from the target class as poison samples, and leverage GNNExplainer, an interpretability method, to find the top-30% unimportant nodes for classification.
- To adapt GFS strategy, we add the cosine modulation to the unimportant node feature and use an amplitude Δ to control its effect. For the rest node features, we add PGD-based adversarial perturbation for suppression.

To adapt UAT to the graph domain, we make the following efforts:

- To align with the original work, we leverage GNNExplainer to find the unimportant nodes for classifying the training graphs from non-target classes. We obtain a trigger pattern by randomly initializing the node features while masking off the other nodes in the graph.
- We denote uniform/targeted adversarial perturbation as **-U** and **-T**, respectively. During testing, we randomly select non-target samples and replace their node features with trigger pattern.

We evaluate the adapted methods and our BA-LOGIC across various graph classification datasets, including MUTAG, PROTEINS, and NCI1 of Morris et al. (2020), and record the results in the following table.

Table 10: Results (ASR|CA(%)) of comparing BA-LOGIC with baselines from image domain.

Datasets	**OPS-GFS**	**UAT-U**	**UAT-T**	**BA-LOGIC**
MUTAG	88.45|60.67	88.91|60.95	90.15|59.45	92.17|61.32
PROTEINS	71.96|70.14	85.73|65.36	86.43|68.18	89.67|71.65
NCI1	83.71|80.65	93.46|77.44	95.17|78.16	94.38|80.39

From Tab. 10, we have the following key findings:

- The adapted methods demonstrate comparable performance in the graph domain, indicating the effectiveness and transferability of their frameworks.
- OPS-GFS uses cosine modulation for the trigger pattern, associated with period T of time series data. While we grid-searched its hyperparameters, lack of knowledge in static graphs potentially limited its performance, especially with multi-class classification on PROTEINS.
- UAT achieves high ASR with both perturbing variants while suffering from slight CA degradation, which is consistent with reports in its original paper.
- UAT can slightly outperform OPS-GFS. We find that UAT can fully use all non-target class samples, while OPS-GFS selects poison samples from a single non-target class due to its original design of binary classification.

Moreover, the additional experiment represents an early adaptation of clean-label backdoors from the image to the graph domain, and we hope the effort can strengthen our contributions.

A.7 ADDITIONAL RESULTS OF ATTACKING AGAINST DEFENDING STRATEGIES

In the main text of our work, we evaluate BA-LOGIC with its ASR when facing defense methods. Due to the space limitation of the main text, we compared our method with three leading competitors against four defense methods on two datasets. In this subsection, we first present the complete comparison with all baselines we select in the main text of our work. We evaluate the ASR of these attack methods against defense models on four datasets, and record the results in Tab. 11. From the table, we obtain similar observations to those in Tab. 6. Compared to competitors, BA-LOGIC still shows significantly higher ASR. Notably, the competitors also achieve better ASR on **Cora** and

Table 11: Results (ASR(%)) of comparing BA-LOGIC with baselines against defense models.

Datasets	Defense	ERBA	ECGBA	EBA-C	GTA-C	DPGBA-C	UGBA-C	BA-LOGIC
Cora	GCN-Prune	5.93	15.56	16.71	15.69	33.10	52.07	**99.17**
	RobustGCN	4.17	14.25	15.28	15.04	21.78	56.09	**99.12**
	GNNGuard	0.00	0.01	0.14	0.00	50.27	35.57	**98.48**
	RIGBD	0.00	0.01	0.00	0.00	0.07	0.16	**95.47**
Pubmed	GCN-Prune	4.13	15.79	19.25	18.95	37.34	59.64	**97.95**
	RobustGCN	2.96	13.24	17.13	18.72	28.13	45.59	**98.10**
	GNNGuard	0.00	0.51	0.00	1.39	41.07	40.58	**95.46**
	RIGBD	0.00	0.01	0.00	0.00	0.01	0.09	**93.01**
Flickr	GCN-Prune	0.00	15.02	16.09	17.19	35.44	54.49	**99.24**
	RobustGCN	0.00	11.25	12.27	15.51	22.26	58.81	**99.02**
	GNNGuard	0.00	0.01	0.00	0.00	53.41	33.14	**99.36**
	RIGBD	0.00	0.01	0.00	0.00	0.07	0.33	**94.86**
Arxiv	GCN-Prune	0.00	13.57	21.07	16.02	17.34	62.31	**96.75**
	RobustGCN	0.00	14.24	17.83	13.29	29.65	44.46	**97.03**
	GNNGuard	0.00	0.51	0.00	0.00	43.77	40.08	**95.37**
	RIGBD	0.00	0.01	0.00	0.00	0.01	0.19	**93.23**

Pubmed than the records of larger graph datasets in Tab. 6, likely due to the graph being of smaller size, aiding in the attack methods generalizing the trigger patterns.

We further analyze why the existing defense methods in Tab. 11 fall short when facing BA-LOGIC. Specifically:

- **GCN-Prune** removes edges between nodes with dissimilar features. Our logic poisoning triggers are generated with the constraint of an unnoticeable limit, which enables our triggers to bypass the defense.
- **RobustGCN** models hidden states of nodes as Gaussian distributions to unweight noisy features and absorb adversarial modifications. Our method explicitly guides the model's inner prediction logic to emphasize the importance of our trigger, instead of identifying our triggers as adversarial.
- **GNNGuard** unweights edges link nodes with low similarity in representation space, effectively acting as an attention-based defense. Our triggers poison the logic of GNNs to be identified as important for prediction, thus forcing GNNGuard to focus on triggers instead of unweighting them.
- **RIGBD** assumes poisoned nodes exhibit high prediction variance, as random edge dropping can remove triggers and change predictions of poisoned nodes back to the original class. Our method adopts a clean-label setting, where the poisoned nodes are originally labeled as the target class without requiring any label alteration. Therefore, removing triggers does not significantly change predictions, causing RIGBD to fail in identifying triggers.

In our work, we employ the black-box threat model, where defense methods can be deployed against unseen target models to counter adversaries. While we note that our method can surpass various defending strategies, including the latest SOTA defense method RIGBD, it is also important to note that the defense methods in our work employ a strong defense goal, which is cleansing the poisoned graph and degrading ASR. The defense goal is reasonable in a real-world scenario, as achieving a weaker defense goal, such as detection, would also lead to the removal of injected triggers naturally.

Meanwhile, we also note that a straightforward and widely adopted defense method is of cleansing graphs by removing edges with unusually high node degrees Dai et al. (2023); Dhali & Dividino (2024). To further demonstrate the robustness of our method, we prune $\{1, 2, 3\}$ edges from nodes with top-5% and top-10% degree after the trigger injection. We propose a metric, Remaining Trigger Connectivity (RTC), defined as the ratio of the number of edges connected to the trigger after pruning to the number before pruning. We evaluate BA-LOGIC under this pruning defense strategy with RTC(%) and ASR | CA (%) on **Arxiv**, and record the results in Tab. 12.

From Tab. 12, we obtain the following key findings:

Table 12: Results of BA-LOGIC against pruning defense strategy.

	Pruning top-5%		Pruning top-10%	
	RTC	ASR | CA	RTC	ASR | CA
Prune 1 edge	96.20	97.45 | 60.42	95.80	97.71 | 61.15
Prune 2 edges	94.80	97.25 | 59.37	91.60	96.82 | 58.72
Prune 3 edges	90.40	96.62 | 56.31	88.70	94.75 | 56.03

- Our approach achieves outstanding performance against this pruning defense method. We owe this to our node selection being of an uncertainty-based rather than a degree-based nature.
- Pruning can defend against backdoor attacks partially, but compromise the clean accuracy of GNN. This is because the optimization of BA-LOGIC is regulated by an unnoticeable constraint in Eq.(8), which ensures the injected trigger maintains high cosine similarity with normal samples.

A.8 ADDITIONAL RESULTS OF MODULE CONTRIBUTION ANALYSIS

A.8.1 HYPERPARAMETER ANALYSIS

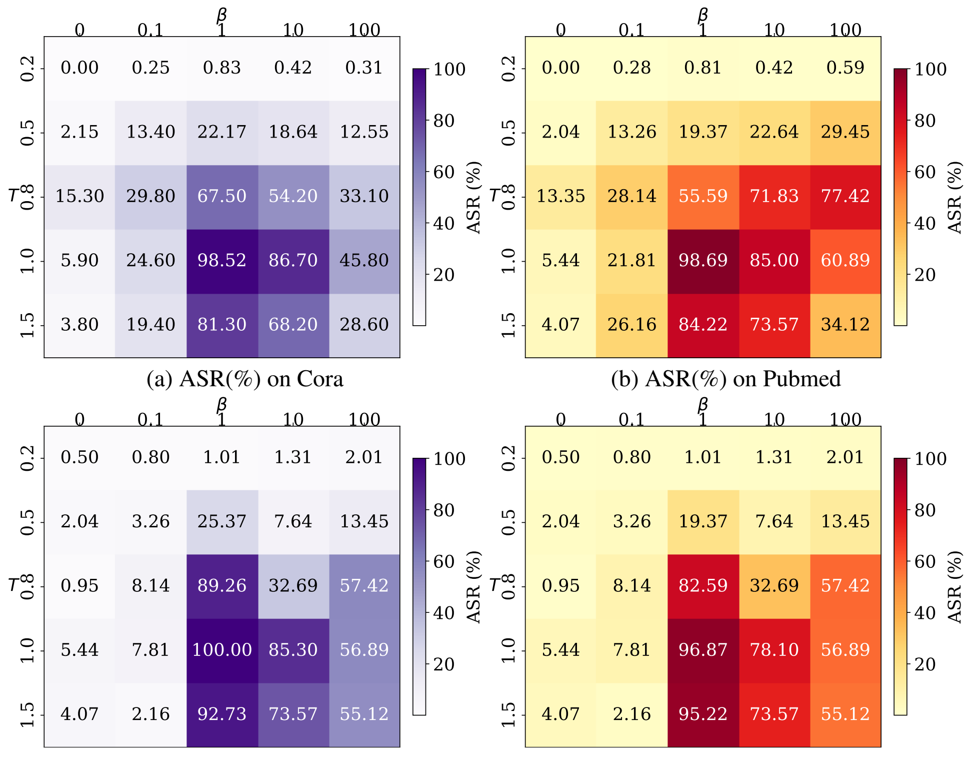

(a) ASR(%) on Cora (b) ASR(%) on Pubmed (c) ASR(%) on Flickr (d) ASR(%) on Arxiv

Figure 7: Hyperparameter sensitivity analysis of BA-LOGIC.

In the main text of our work, we introduce hyperparameters to regulate the magnitude of the logic poisoning loss during optimization. To thoroughly understand their impact, we further investigate how the main hyperparameters, i.e., T in Eq.(7) and β in Eq.(10), affect the performance of BA-LOGIC. Specifically, T controls the expected margin of importance scores between trigger nodes and clean neighbor nodes. And β controls the weight of logic poisoning loss, respectively. To explore the effects of T and β, we take the value of T and β corresponding to the experimental result of Tab. 3 as the normalized 1 and conduct parameter sweeps. Specifically, we vary T as $\{0.2, 0.5, 0.8, 1.0, 1.5\}$. And β is changed from $\{0, 0.1, 1, 10, 100\}$. We report the ASR of attacking a 2-layer GCN in Fig. 7, from which we observe: **(i) Arxiv** requires larger trigger margins T than **Pubmed**, due to its higher average node degree, where clean neighbor nodes exert stronger influence on predictions. Hence, higher margins T and weights β are necessary to avoid attack failure. In practice, the value of T is often taken as the local maximum of the gradient of the trigger nodes to ensure attack effectiveness. **(ii)** ASR degrades when T and β are overly high. This is because unsuitable large values of T and β could hinder the optimization of BA-LOGIC.

A.8.2 CROSS-METHOD MODULE UTILITY ANALYSIS

In the main text of our work, we have emphasized that one challenge of clean-label graph backdoor attack facing is that the trigger-attached poisoned samples are correctly labeled as the target class. Thus, the injected triggers would be treated as irrelevant information in prediction, resulting in poor backdoor performance.

To address the challenge, we deliberately select the nodes with high uncertainty because:

- These nodes exhibit irregular patterns that are weakly associated with the target class y_t
- The triggers obtained by the generator exhibit consistent patterns to poison the prediction logic, causing the model to shift focus from irregular patterns to treating these triggers as key features

Specifically, we design an uncertainty metric based on two aspects: **(i)** the probability of being predicted as the target class is low, and **(ii)** the node is also uncertain for other classes.

As we stated in our work, the main purpose of poison node selection is more efficient usage of attack budget, and our main contribution lies in inner logic poisoning, rather than the poison node selection. Poisoned node selection serves solely as positions for trigger injection. After injecting the triggers, the target model trained on the backdoored graph is backdoored, and any test node could be successfully attacked by attaching triggers during the inference of the target model. Indeed, we randomly selected 25% of test nodes as the target for each evaluation.

In our original comparison, we faithfully preserved each method's specific poison node selection, either designed or random. While it ensures a fair comparison, we agree on that evaluate the performance of baselines when they also poison nodes that are selected by our poisoned node selector would highlight the module utility. Hence, we update baselines with our poison node selection under clean label setting, and denote the updated methods with **-S**. We evaluate them on four datasets and record the average ASR|CA(%) towards three target models adopted in the main text of our work, i.e., GCN, GIN, and GAT:

Table 13: Comparison between BA-LOGIC and poisoned node selection updated baselines.

Dataset	ERBA-S	EBA-S	ECGBA-S	GTA-S	UGBA-S	DPGBA-S	BA-Logic
Cora	21.81 | 80.90	33.25 | 72.62	56.84 | 79.28	32.52 | 80.92	68.94 | 81.94	67.87 | 81.88	98.20 | 83.72
Pubmed	22.95 | 85.69	33.99 | 85.50	58.38 | 85.03	41.57 | 86.10	68.87 | 85.82	70.31 | 85.61	96.89 | 85.79
Flickr	4.70 | 46.29	34.15 | 44.99	62.08 | 44.99	51.71 | 45.88	68.08 | 45.66	71.39 | 44.78	99.90 | 45.70
Arxiv	0.01 | 65.43	31.09 | 65.57	54.94 | 64.21	37.98 | 65.79	70.79 | 66.08	69.10 | 66.27	98.03 | 66.02

From Tab. 13, we obtain the following key findings:

- All baselines show enhanced ASR when using our poison node selection, confirming its effectiveness
- Among them, ECGBA-S has the most significant improvement. It is because we improved its uncertainty metric, so the node should also be uncertain for other classes
- Methods that select nodes randomly only achieve limited improvement, such as ERBA and DPGBA, indicating that the trigger is paramount for effective graph backdoor

Results from this analysis demonstrate two main conclusions: **(i)** Our poisoned node selection module is effective and generalizable, as its adoption improves the performance of baselines. **(ii)** However, the primary source of our method's superior attack success rate is the logic poisoning mechanism with solid theoretical ground. This is evidenced by the fact that updated baselines still fail to compare with our method.

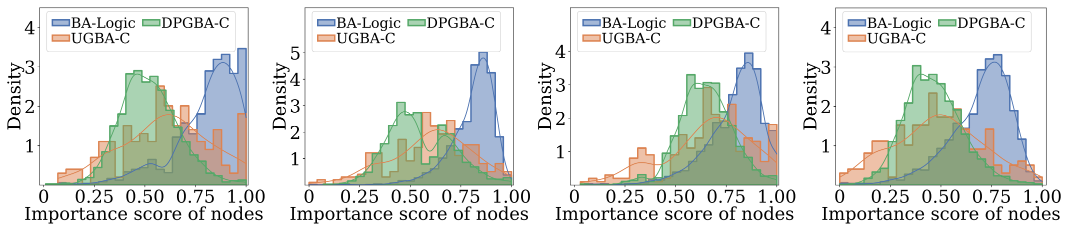

(a) Cora (b) Pubmed (c) Flickr (d) Arxiv

Figure 8: Comparison of IRT distribution.

A.9 Additional Analysis on IRT and Impact of Attack Budget

Important Scores of Trigger Nodes In our preliminary analysis, we conduct a theoretical analysis to show that the existing methods fail under clean-label settings because their triggers are deemed unimportant for prediction by the target GNN models. We further reveal that the attack success rate is bounded by the important rate of triggers, a novel metric proposed in our preliminary analysis. However, there is still a research question waiting to be addressed: Does BA-LOGIC successfully poison the target GNNs' prediction logic as designed? To answer this question, we employ GNNExplainer to measure trigger importance scores distribution for poisoned nodes, comparing BA-LOGIC against two leading baselines, UGBA-C and DPGBA-C.

The histograms of the normalized importance scores across four datasets, **Cora**, **Pubmed**, **Flickr**, and **Arxiv**, are presented in Fig. 8. For each dataset, we report the IRT distributions averaged over the three clean models in Tab. 3, i.e., GCN, GIN, and GAT. From these figures, we have the following key observations:

- **BA-LOGIC** shows concentration of nodes with large IRT values, with peaks close to the maximal importance score. This indicates that the logic poisoning triggers are identified as important by the logic of backdoored GNNs.
- **UGBA-C and DPGBA-C** exhibit flatter IRT distributions, with most mass in the lower importance range. This indicates that their triggers are less effective at poisoning the inner logic of the target models.
- Across all four datasets and three clean models, methods with higher IRT consistently achieve higher ASR. This is aligned with theoretical analysis, which indicates existing graph backdoor methods generally lead to a low important rate of triggers, resulting in poor attack performance under the clean-label setting.

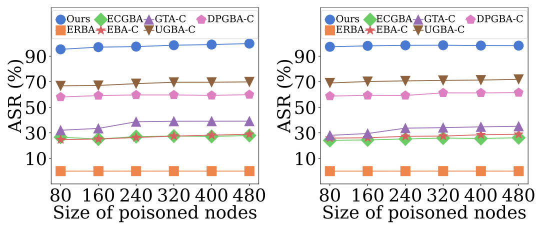

(a) GCN (b) GAT

Figure 9: Impact of attack budget.

Impact of Attack Budget In our preliminary analysis, we evaluate BA-LOGIC and competitors by varying the size of poisoned nodes $\mathcal{V}_P$, which is also the attack budget of backdoor attack. Here, we further explore the attack performance with various attack budgets. Specifically, we vary the size of $\mathcal{V}_P$ as $\{80, 160, 240, 320, 400, 480\}$, and record the results on **Arxiv** with GCN and GAT in Fig. 9, from which we observe: **(i)** ASR of most competitors increases with the increase of $\mathcal{V}_P$, which intuitively satisfies expectations. BA-LOGIC consistently outperforms the baselines regardless the size of $\mathcal{V}_P$, showing its effectiveness. Notably, the gaps between our method and baselines widen when the budget is smaller, demonstrating the effectiveness of the poisoned node selection in effectively utilizing the attack budget. **(ii)** Compared to other competitors, the ASR of BA-LOGIC remains stable across GNN models with distinct inner logic, showing BA-LOGIC's transferability.

We further investigate the impact of a smaller attack budget. Specifically, we conducted additional evaluations for EBA-C, UGBA-C, and DPGBA-C with attack budget ranges from $\{10, 20, 30, 40, 50\}$. We evaluate these methods on **Cora** and **Pubmed**, and record ASR | CA(%) as below:

From Tab. 14, we have the following key findings:

Table 14: Results (ASR | CA(%)) on **Cora** and **Pubmed** with less attack budget.

	Cora				**Pubmed**			
Δ_P	**EBA-C**	**UGBA-C**	**DPGBA-C**	**BA-Logic**	**EBA-C**	**UGBA-C**	**DPGBA-C**	**BA-Logic**
10	5.13 | 82.47	15.29 | 81.05	17.87 | 80.95	65.16 | 83.11	0.69 | 86.38	11.89 | 85.36	21.15 | 84.95	62.07 | 85.32
20	12.39 | 82.78	51.26 | 80.14	45.43 | 81.36	87.13 | 83.06	8.61 | 86.21	34.62 | 85.36	49.31 | 84.36	88.04 | 85.09
30	15.64 | 82.34	62.20 | 80.65	50.77 | 80.44	92.17 | 82.39	19.47 | 86.75	64.16 | 85.05	54.61 | 85.44	94.79 | 84.67
40	29.03 | 81.86	63.18 | 80.37	51.03 | 80.85	94.22 | 83.16	29.76 | 85.33	64.07 | 85.16	55.57 | 85.85	95.44 | 84.96
50	29.17 | 80.99	63.23 | 79.85	51.15 | 80.75	96.05 | 81.85	30.66 | 85.17	63.97 | 85.25	57.86 | 85.75	95.71 | 85.05

- Our method exhibits leading performance against all baselines, and all methods demonstrate slightly better CA with less attack budget.
- The relationship between ASR and attack budget is nonlinear, and ASR tends to show more obvious improvements when the attack budget increases from a smaller value.

B Time Complexity Analysis

In BA-Logic, the time complexity mainly comes from the logic poisoning sample selection and the bi-level optimization of the logic poisoning trigger generator. Let h denote the embedding dimension. The cost of the logic poisoning node selection can be represented approximately as $O(Mdh|\mathcal{V}|)$, where d is the average degree of nodes and M is the number of training iterations for the pre-trained GCN model, which is small. The cost of bi-level optimization consists of updating the weight of the surrogate GNN model in inner iterations and updating the logic poisoning trigger generator in outer iterations. The cost for updating the surrogate model is approximately $O(Ndh|\mathcal{V}_P|)$, where d is the average degree of nodes and N is the number of inner training iterations for the surrogate GNN model. For the trigger generator, the classification loss and prediction logic poisoning loss are computed with cost as $O(2dh|\mathcal{V}|)$. For the unnoticeable loss $\mathcal{L}_U$, its time complexity is $O(hd|\mathcal{V}_p|\Delta_g)$. Hence, the overall time complexity of each iteration of bi-level optimization is $O(dh(2|\mathcal{V}| + (\Delta_g + N)|\mathcal{V}_P|)$, which is linear to the size of the graph. Hence, BA-Logic can efficiently poison the inner prediction logic of target models for clean-label graph backdoor attacks.

C Implementation Details

C.1 Datasets Statistics

In the main text of our work, we select extensive public real-world graph datasets to evaluate our methods. These graph datasets are diverse in sources, scales, heterophily, tasks, etc. The detailed statistics of these graph datasets are presented in Tab. 15.

Table 15: The statistics of datasets in our work.

Datasets	**#Nodes**	**#Edges**	**#Graphs**	**#Features**	**#Classes**
Cora	2,708	5,429	1	1,433	7
Pubmed	19,717	44,338	1	500	3
Flickr	89,250	899,756	1	500	7
Arxiv	169,343	1,166,243	1	128	40
CS	18,333	163,788	1	6,805	15
Physics	34,493	495,924	1	8,415	5
Squirrel	5,201	217,073	1	2,089	5
Chameleon	2,277	36,101	1	2,325	5
Penn	41,554	1,362,229	1	5	2
Genius	421,961	984,979	1	12	2
Products	2,449,029	61,859,140	1	100	47
MUTAG	~17.9	~39.6	188	7	2
NCI1	~29.8	~32.3	4110	-	2
PROTEINS	~39.1	~145.6	600	3	6

C.2 Details of Compared Methods

In the main text of our work, we compare BA-LOGIC with representative and state-of-the-art graph backdoor attack methods, such as **DPGBA-C** Zhang et al. (2024b), and **UGBA-C** Dai et al. (2023). These methods originally required altering the labels of poisoned nodes. In our experiments, they are extended to the clean-label setting by only selecting poisoned nodes of the target class. We also compare with **ERBA** Xu & Picek (2022), and **ECGBA** Fan & Dai (2024), which are the latest graph backdoor attacks for clean-label settings. We further extend the comparison with our method to **SCLBA** Dai & Sun (2025), **GCLBA** Meguro et al. (2024), **TRAP** Yang et al. (2022) for graph classification; and include **SNTBA** Dai & Sun (2024), **PSO-LB** and **LB** Zheng et al. (2023) for edge prediction. For a fair comparison, hyperparameters of the methods are fine-tuned based on the performance of the validation set. The details of the compared methods are described as follows:

- **ERBA** Xu & Picek (2022): It is the early work among the initial clean-label backdoor attacks on GNNs. ERBA tailors graph classification tasks, samples training graphs randomly as targets, and generates Erdös–Rényi random graphs as triggers. ERBA can also be considered a straightforward variant of SBA Zhang et al. (2021). To adapt ERBA to the settings of our work, we maintain a fixed node size of three within the random graph and select poisoned nodes from training nodes belonging to the target class. All other settings remain consistent with those described in the original work.
- **EBA** Xu et al. (2021): It is the first explainability-based graph backdoor attack. EBA aims to conduct a graph backdoor attack on both node classification and graph classification tasks. For the graph classification task, EBA selects the least important nodes as trigger injecting positions based on the node importance matrix generated by GNNExplainer. Thus, EBA can remain unnoticeable to some extent. For the node classification task, EBA selects the most important node features based on the node importance matrix generated by GraphLIME Huang et al. (2022) and manipulates them as trigger features. To adapt EBA to the settings of our work, we employ GNNExplainer to select the most representative nodes from the target class without altering their labels. The trigger is an Erdös-Rényi random graph with a density of $\rho = 0.8$, as in the original work. All other settings remain consistent with those described in the original work.
- **ECGBA** Fan & Dai (2024): This is one of the latest clean-label graph backdoor attacks focused on node classification. ECGBA completes the graph backdoor attack by coordinating a poison node selector and a trigger generator. It selects nodes that are misclassified as target classes by surrogate GCN as poison nodes, thereby improving performance to a certain extent. However, it should be noted that ECGBA does not consider the inner prediction logic of the target model, and for efficiency, ECGBA's trigger only contains one node, which limits its effect. To adapt ECGBA to the settings of our work, we select poisoned nodes from training nodes belonging to the target class. All other settings remain consistent with those described in the original work.
- **GTA** Xi et al. (2021): GTA selects poisoned nodes randomly but adopts a trigger generator to inject subgraphs as node-specific triggers. The trigger generator is purely optimized by the backdoor attack loss with no constraints. To adapt GTA to the settings of our work, we prohibit GTA from modifying the labels of poisoned nodes and select poisoned nodes from training nodes belonging to the target class. All other settings remain consistent with those described in the original work.
- **UGBA** Dai et al. (2023): It is the state-of-the-art backdoor attack on GNNs. UGBA adopts a representative node selector to utilize the attack budget fully. An adaptive trigger generator is optimized with constraint loss to ensure the generated triggers are unnoticeable. To adapt UGBA to the settings of our work, we prohibit UGBA from modifying the labels of poisoned nodes and select poisoned nodes from training nodes belonging to the target class. All other settings remain with those described in the original work.
- **DPGBA** Zhang et al. (2024b): Except for the node selector and trigger generator, DPGBA adopts an out-of-distribution detector to ensure the attributes of triggers within the distribution and thus achieve unnoticeable attacks. To adapt DPGBA to the settings of our work, we prohibit DPGBA from modifying the labels of poisoned nodes and select poisoned nodes from the target class. All other settings remain consistent with those described in the original work.
- **SCLBA** Dai & Sun (2025): SCLBA is one of the latest clean-label graph backdoor attacks on GNNs for graph classification. SCLBA leverages node semantics by using a specific, naturally occurring type of node as a trigger. Its core design involves selecting semantic trigger nodes based

on a node importance analysis using degree centrality, followed by injecting these triggers into a subset of target class graph samples. To adapt SCLBA to the settings of our work, we select poisoned graphs from training graphs from the target class. All other settings remain consistent with those described in the original work.

- **GCLBA** Meguro et al. (2024): GCLBA is a gradient-based clean-label graph backdoor attack for graph classification. GCLBA comprises two main phases: graph embedding-based pairing and gradient-based trigger injection. The pairing phase establishes relationships between graphs from the target and other classes based on distance in the embedding space, selecting targets far from the decision boundary. The trigger injection phase embeds tailored edges as triggers into paired graphs based on gradient. To adapt GCLBA to the settings of our work, we select poisoned graphs from training graphs from the target class. All other settings remain consistent with those described in the original work.
- **TRAP** Yang et al. (2022): TRAP is a clean-label graph backdoor attack for graph classification. TRAP generates structure perturbation as triggers without a fixed pattern. TRAP adopts the same black-box setting as SCLBA, achieved by exploiting a surrogate GCN model to generate perturbation triggers via a gradient-based score matrix. To adapt TRAP to the settings of our work, we select poisoned graphs from training graphs from the target class. All other settings remain consistent with those described in the original work.
- **SNTBA** Dai & Sun (2024): SNTBA proposes a backdoor attack targeting GNN models in edge prediction tasks. SNTBA uses a single node as the backdoor trigger, and the backdoor is injected by poisoning selected unlinked node pairs in the training graph. SNTBA injects the trigger to both nodes in the pairs and links them, showing a more relaxed threat model. During inference, the backdoor is activated by linking the trigger node to the two end nodes of unlinked target node pairs in the test graph. The attacked GNN model would incorrectly predict that a link exists between the unlinked target node pairs. To adapt SNTBA to the settings of our work, we select poisoned nodes from training nodes of the target class and prohibit SNTBA from modifying the link state. All other settings remain consistent with those described in the original work.
- **LB** Zheng et al. (2023): LB is a backdoor attack method for edge prediction. LB utilizes a subgraph as trigger, combining fake/injection nodes with the nodes of the target link. The initial trigger is a random graph comprising two injection nodes and the two target link nodes. LB optimizes triggers by gradient generated by an edge prediction GNN model, aiming to minimize the attack objective loss, i.e., L2 distance between prediction and the attacker-chosen target link state T. The trigger is iteratively updated based on the gradient direction. LB requires modifying the target link state embedded with the trigger to T. LB supports white-box and black-box attack scenarios, where the latter utilizes a surrogate model. To adapt LB to the settings of our work, we select poisoned nodes from training nodes of the target class and prohibit LB from modifying the link state. All other settings remain consistent with those described in the original work.
- **PSO-LB** Zheng et al. (2023): PSO-LB is a variant proposed for comparison in the original work of LB. It utilizes particle swarm optimization Kennedy & Eberhart (1995) to modify the injection node features and structure of the trigger. To adapt PSO-LB to the settings of our work, we select poisoned nodes from training nodes of the target class and prohibit PSO-LB from modifying the link state. All other settings remain consistent with those described in the original work.

C.3 Other Implementation Details

Our implementation is based on PyTorch 2.1.0 and PyTorch Geometric 2.4.0. All the experiments are evaluated on an NVIDIA A100 GPU with 80 GB of memory. The detailed architecture of our method is described as follows. *Firstly*, the framework of BA-LOGIC consists of the following modules:

- A 2-layer GCN as the surrogate model.
- A 2-layer GCN as the pre-trained poisoned node selector.
- A 2-layer MLP as the logic-poisoning trigger generator.

Secondly, for each architecture of GNN models, we fix the hyperparameters of BA-LOGIC as follows:

- Target class: 0
- Trigger size: 3.

- Number of GNN layers L: 2.
- Hidden dimension H: 32.
- Weight decay: $5e-3$.
- Learning rate: $1e-2$.
- Seeds of NumPy, Torch, and CUDA: 3407.
- Activation function: ReLU for GCN and GIN, ELU for GAT.
- Mixed precision training is enabled for speeding up.

Thirdly, the two hyperparameters β and T are selected based on the grid search on the validation set. Specifically, T is set as $\{32, 32, 64, 72\}$ and β is set as $\{0.8, 0.8, 1.0, 1.2\}$ for **Cora**, **Pubmed**, **Flickr** and **Arxiv**, respectively.

In practice, we split the graph into training, validation, and test sets with a ratio of 25%/25%/50%. We set the training epoch for the surrogate GCN and the logic-poisoning trigger generator as 200 for all datasets, and we vary the attack budget Δ_P on the number of $\mathcal{V}_P$ as $\{100, 100, 200, 200\}$ for **Cora**, **Pubmed**, **Flickr**, and **Arxiv**, respectively.

Table 16: Comparisons of dataset node size and method training time.

Dataset	**#Nodes**	**UGBA**	**DPGBA**	**BA-LOGIC**
Flickr	89,250	32.0s	57.7s	123.4s
Arxiv	169,343	51.3s	68.9s	155.7s

In our empirical experiments conducted on large-scale graph datasets such as **Flickr** and **Arxiv**, which comprise 89,250 and 169,343 nodes respectively, we set the size of $\mathcal{V}_P$ as 200 on average and still achieve a much higher ASR than other competitors. We also report the overall training time cost of BA-LOGIC compared with UGBA and DPGBA on the **Flickr** and **Arxiv** datasets in Tab. 16. The results are consistent with the time complexity analysis in Appendix B, indicating that the BA-LOGIC requires only approximately 60 seconds more training time than the two most powerful competitors on a larger graph. The additional time is acceptable given that our BA-LOGIC achieves an ASR over 90%, while these competitors achieve an ASR over 60%. This demonstrates that BA-LOGIC effectively generates triggers that the target model memorizes quickly by poisoning the inner logic, highlighting its potential in scalability.

D RELATED WORKS

Graph Neural Networks Graph Neural Networks (GNNs) come into the spotlight due to their remarkable ability to model graph-structured data Chen et al. (2020); Hamilton et al. (2017); Kipf & Welling (2017); Gasteiger et al. (2019); Veličković et al. (2018); Wu et al. (2019). Recently, many GNN models have been proposed to further improve the performance of GNNs Dai et al. (2024). There are also works that address the fairness Dai & Wang (2021a), robustness Wang et al. (2023); Dai et al. (2022a), and explainability Pope et al. (2019); Dai & Wang (2021b) challenge of diverse GNN models. And GNN models for handling heterophilous graphs, in which connected nodes may in fact have distinct attributes Luan et al. (2022), are also proposed Zhang et al. (2019); Lim et al. (2021). While the representational powers of GNN models have been well studied, GNN models' performance under diverse backdoor attacks has remained largely an open question, particularly performance under clean-label settings Zhang et al. (2021). Our analysis reveals that the crux of GNNs' vulnerability to backdoor attacks lies in whether their prediction logic is affected by the backdoor patterns. Based on this, we propose a novel framework to address this open question.

Graph Backdoor Attacks Exploring backdoor attacks on graphs has aroused increasing interest among the graph learning community Zhang et al. (2021); Xi et al. (2021); Dai et al. (2023); Xu & Picek (2022); Zhang et al. (2024b). A large body of research focuses on enhancing graph backdoor attacks via generating the adaptive triggers under the general dirty-label settings Xi et al. (2021), and some of them point out the importance of remaining unnoticeable from the perspective of similarity Dai et al. (2023) and distribution Zhang et al. (2024b). For the clean-label graph backdoor attack, some initial efforts Xu & Picek (2022); Xing et al. (2024); Chen & Zhou (2024); Dai & Sun (2025) have been proposed to harness significant node features for trigger design. ERBA Xu & Picek (2022) proposes to conduct the graph backdoor attack under clean-label settings. However, its discussions focus on graph classification as a downstream task, which differs from node classification as the node instances are, in fact, interdependent in the latter downstream task Hu et al. (2020). Moreover, ERBA generates Erdös–Rényi random graph Erdos et al. (1960) to act as triggers, showing limited exploration from the effectiveness perspective. EBA Xu et al. (2021), CGBA Xing et al. (2024), and EGNN Wang et al. (2024a) conduct the graph backdoor attack for node classification by changing part of the most representative node features as a trigger instead of injecting a subgraph containing nodes. Similarly, clean-label graph backdoor attack methods for graph classification by manipulating the edges as a trigger are also proposed Yang et al. (2022); Meguro et al. (2024). However, modifying the present feature or structure in the graph is generally unrealistic for graph backdoor injection. For instance, in social or transaction networks, attackers could easily register malicious users and build connections with other users, while modifying existing users' attributes or connections that are well-preserved, is much harder to achieve Alothali et al. (2018). There is also concurrent work Xia et al. (2025) that proposes to address the failure of existing clean-label graph backdoor attacks, which boosts the classification confidence of trigger-attached samples towards the target class. In general, the existing works differ fundamentally from our method, which achieves logic poisoning that explicitly makes the trigger's importance score to exceed that of clean nodes by a predefined margin, enforcing the target model to deem our triggers as essential for its prediction. Our method addresses a novel problem to poison the inner prediction logic of GNNs for an effective clean-label graph backdoor attack.

Explaining the Prediction Logic of GNNs To enhance the trustworthiness of the predictions made by GNNs, researchers have made extensive attempts to develop explanation methods for GNN models Huang et al. (2022); Schnake et al. (2021); Luo et al. (2020). GNNExplainer Ying et al. (2019) is proposed to leverage mutual information to find a compact subgraph with the most related features for interpreting the prediction of a node or graph being explained. The work of Pope et al. (2019) proposes a variant of Grad-CAM Selvaraju et al. (2017) towards GNNs, which identifies important and class-specific features at the last convolutional layer. π-GNN Yin et al. (2023) is one of the state-of-the-art explanation methods that distill the universal interpretability of GNNs by pre-training over synthetic graphs with ground-truth explanations. Research on explaining makes the prediction logic of GNNs traceable, which in turn helps researchers to understand the behaviors of GNNs (Zhang et al., 2024a; Dai et al., 2024). Many works have been proposed to enhance GNNs from an explainability perspective, enabling them to provide accurate predictions and faithful explanations simultaneously Wang et al. (2024b); Tang et al. (2023). In contrast, while explainability-enhanced graph backdoor attacks Xu et al. (2021); Wang et al. (2024c;a) are still in their nascent stages, there is even less attention paid to focus on the clean-label graph backdoor attack, highlighting a gap that our method aims to address.

E Threat Model Level Comparison

In the main text of our work, we introduced the threat model of BA-LOGIC in Sec. 2.1. To highlight the fairness of the comparison between our method and the included baselines, we further present a more comprehensive threat model level comparison.

In general, our method adopts a threat model that has stricter limitations than most existing graph backdoor attacks. Specifically, we assume the attacker's capability is limited to:

- The attacker **can NOT** remove or manipulate the existing nodes and edges in the training graph.
- The attacker **can NOT** alter the labels of the training data.
- The attacker **can NOT** know the information of the target model, such as parameters or gradients.
- The attacker **can NOT** either know or control the defending by data cleaning. Moreover, we demonstrate the effectiveness of BA-LOGIC against defenders that prune malicious nodes and edges in Sec. 5.4.
- The attacker **can ONLY** inject a small number of triggers to the training nodes. Each trigger is subjected to strict limits on size.

Table 17: Threat model level comparison.

Method	Manipulates Existing Nodes/Edges	Alters Training Labels	Knows/Controls Defense for Data Cleaning	Trigger Injection	Comparison to Ours
GTA	✗	✓	✗	✓	Stronger assumption than ours
UGBA	✗	✓	✗	✓	Stronger assumption than ours
DPGBA	✗	✓	✗	✓	Stronger assumption than ours
TRAP	✓	✓	✗	✗	Stronger assumption than ours
EBA	✓	✗	✗	✗	Stronger assumption than ours
CGBA	✓	✗	✗	✗	Stronger assumption than ours
SCLBA	✓	✗	✗	✗	Stronger assumption than ours
GCLBA	✓	✗	✗	✗	Stronger assumption than ours
SNTBA	✓	✓	✗	✓	Stronger assumption than ours
LB	✓	✓	✗	✓	Stronger assumption than ours
ERBA	✗	✗	✗	✓	Same
ECGBA	✗	✗	✗	✓	Same
Our BA-Logic	✗	✗	✗	✓	–

For the attacker's knowledge, our threat model is in line with the commonly adopted black-box graph backdoor attacks. Specifically, we assume that:

- The attacker **can NOT** know target GNN's architecture and hyperparameters. As stated in Sec. 2.1, we adopt a strict black-box setting where the attacker can only employ a surrogate model and transfer the attack to the unseen target model for evaluation.
- The attacker **can ONLY** know partial training data of the target GNN. This widely adopted assumption is reasonable. For example, when a GNN is trained on data from Twitter, much of that data is publicly accessible and can be readily crawled by an attacker.

We further summarize a threat model comparison of our method with existing graph backdoor attacks in Table 17 to highlight the fairness of our comparison, from which we highlight that:

- Our BA-Logic does not enable training label altering, which imposes a stricter limitation and weaker assumption compared to general backdoor attacks.
- Some clean backdoor attacks obtain triggers by altering existing nodes or edges, which is less practical than trigger injection. For instance, in social or transaction networks, attackers could easily register malicious users and build connections with other users. However, modifying the attributes or connections of existing users, which are well-preserved, is much harder to achieve in practice.
- Our BA-Logic adopts the same threat model as two recently proposed clean-label backdoor methods, i.e., ERBA and ECGBA. This alignment ensures our method is evaluated under a contemporary and practical threat model, facilitating a fair and relevant comparison.

F Optimization Algorithm

We present the algorithm for solving the bi-level optimization problem in Eq. (10).

Lower-Level Optimization In the lower-level optimization, the surrogate GNN is trained on the backdoored dataset. To reduce the computational cost, we update surrogate model θ for N inner iterations with fixed θ_g to approximate θ^*:

$$\theta^{n+1} = \theta^n - \alpha_f \nabla_\theta \mathcal{L}_f(\theta, \theta_g), \tag{15}$$

where θ^n denotes model parameters after $n-$th iterations. α_s is the learning rate for training the surrogate model.

Upper-Level Optimization In the outer iteration, the updated surrogate model parameters θ^N are used to approximate θ^*. Moreover, we apply a first-order approximation in computing gradients of

Algorithm 1 Algorithm of BA-LOGIC

```
Require: $\mathcal{G} = (\mathcal{V}, \mathcal{E}, \mathbf{X})$, $\mathcal{Y}_L$, $\beta$, $T$.
Ensure: Backdoored graph $\mathcal{G}_B$, trained trigger generator $f_g$
 1: Initialize $\theta$ and $\theta_g$ for surrogate model $f$ and logic poisoning trigger generator $f_g$, respectively;
 2: Select logic poisoning nodes set $\mathcal{V}_P$ based on Eq.(4) ;
 3: while not converged yet do
 4:     for $t = 1, 2, \ldots, N$ do
 5:         Update $\theta$ by descent on $\nabla_\theta \mathcal{L}_f$ based on Eq.(15) ;
 6:     end for
 7:     Update $\theta_g$ by descent on $\nabla_{\theta_g}(\sum l(\cdot) + \mathcal{L}_U + \beta\mathcal{L}_A)$ based on Eq.(16);
 8: end while
 9: for $v_i \in \mathcal{V}_P$ do
10:     Generate the trigger $g_i$ for $v_i$ by using $f_g$;
11:     Update $\mathcal{G}_B$ based on $a(\mathcal{G}_B^i, g_i)$;
12: end for
13: return $\mathcal{G}_B$, and $f_g$;
```

θ_g to reduce the computation cost further:

$$\theta_g^{k+1} = \theta_g^k - \alpha_g \nabla_{\theta_g}\big(\sum_{v_i \in \mathcal{V}} l(f_{\bar{\theta}}(\tilde{v}_i(\theta_g)), y_t) + \mathcal{L}_U(\theta_g) + \beta\mathcal{L}_A(\bar{\theta}, \theta_g)\big), \tag{16}$$

where $\bar{\theta}_s$ indicates the parameters when gradient propagation stopping. α_g is the learning rate of the training trigger generator. The training algorithm and time complexity analysis of BA-LOGIC are given in Appendix G and Appendix B, respectively.

G TRAINING ALGORITHM

We formalize the training algorithm of BA-LOGIC in Algorithm 1. In line 2, we first select the poisoned nodes $\mathcal{V}_P$ with the top-Δ_P highest scores calculated by Eq.(4). From line 3 to line 9, we train the trigger generator f_g by solving a bi-level optimization problem based on Eq.(10). In detail, we update the lower-level optimization (line 5) to poison the target model's inner logic and the outer-level optimization (line 7) to update trigger generator f_g, respectively. These goals are achieved by doing gradient descent on θ and θ_g based on Eq.(15) and Eq.(16). From line 10 to line 13, we use the well-trained f_g to generate triggers for each poisoned node $v_i \in \mathcal{V}_P$ and update $\mathcal{G}$ to obtain the backdoored graph $\mathcal{G}_B$.

After presenting the training algorithm of BA-LOGIC, we analyze the time complexity of BA-LOGIC in Appendix B.

H THEORETICAL ANALYSIS

In the main text of this work, we conclude that the failure of existing clean-label graph backdoors stems from the target model's inability to treat the trigger as a critical factor influencing classification outcomes. To rigorously analyze the failure mechanism of existing clean-label graph backdoor methods, we conduct a theoretical analysis in Sec. 2.3. Here we provide the proof.

Assumptions on Graphs Following Dai et al. (2023); Zhang et al. (2025), we consider a graph $\mathcal{G}$ where (i) The node feature $\mathbf{x}_i \in \mathbb{R}^d$ is sampled from a specific feature distribution F_{y_i} that depends on the node label y_i. (ii) Dimensional features of $\mathbf{x}_i$ are independent to each other. (iii) The magnitude of node features is bounded by a positive scalar vector S, i.e., $\max_{i,j} |\mathbf{x}_i(j)| \leq S$.

These assumptions are reasonable in the context of graph representation learning for the following reasons:

- **Label-correlated feature distributions (Assumption i)**: In graph-structured data, node features often exhibit strong correlations with their labels. For instance, in an academic collaboration network, researchers' publication keywords (features) naturally reflect their disciplinary domains (labels) through semantic correspondence;

- **Independence of feature dimensions (Assumption ii)**: In many real-world graph datasets, especially the high-dimensional ones, the correlations between features are typically weak or statistically insignificant.
- **Boundaries of features (Assumption iii)**: Feature magnitudes are often bounded due to practical constraints in real-world data. Moreover, common techniques such as normalization or standardization during pre-processing can effectively bound them within a certain range.

Theorem 1. *We consider a graph $\mathcal{G} = (\mathcal{V}, \mathcal{E}, \mathbf{X})$ follows Assumptions. Given a node v_i with label y_i, let deg_i be the degree of v_i, and γ be the value of the important rate of trigger. For a node v_i attached with trigger g_i, the probability for GNN model f predict v_i as target class y_t is bounded by:*

$$\mathbb{P}(f(v_i) = y_t) \leq 2d \cdot \exp\left(-\frac{deg_i \cdot (1-\gamma)^2 \cdot \|\mu_{y_t} - \mu_{y_i}\|_2^2}{2d \cdot S^2}\right), \tag{17}$$

where d is the node feature dimension, μ_{y_t} and μ_{y_i} are the class centroid vectors in the feature space for y_i and y_t, respectively.

Proof. We present the pre-activated node representation as $\mathbb{E}[\mathbf{h}_i] = \mathbb{E}[\sum_{j \in \mathcal{N}(i)} \frac{1}{\sqrt{\deg_i}\sqrt{\deg_j}} \mathbf{W}\mathbf{x_j}]$. Following the Assumption (ii), $\mathbb{E}[\mathbf{h}_i]$ can be written as:

$$\begin{aligned} \mathbb{E}[\mathbf{h}_i] &= \mathbb{E}\left[\sum_{j \in \mathcal{N}(i)} \frac{1}{\sqrt{\deg_i}\sqrt{\deg_j}} \mathbf{W}\mathbf{x}_j\right] \\ &= \sum_{v_j \in \mathcal{N}_c(i)} \frac{1}{\sqrt{\deg_i}\sqrt{\deg_j}} \mathbf{W}\mathbb{E}[\mathbf{x}_j] + \sum_{v_k \in \mathcal{N}_g(i)} \frac{1}{\sqrt{\deg_i}\sqrt{\deg_k}} \mathbf{W}\mathbb{E}[\mathbf{x}_k], \end{aligned} \tag{18}$$

Let $\alpha_{ij} = \frac{1}{\sqrt{\deg_i}\sqrt{\deg_j}}$ denotes the normalized aggregation weight. To get a tighter bound, we assume that the clean neighbor nodes of v_i are labeled as y_i, and the neighbor node within the trigger is already considered important by an arbitrary graph explainer for the prediction of v_i. Moreover, following Dai et al. (2022b); Zhang et al. (2025), we consider a regular graph $\mathcal{G}$, i.e., each node has the same number of neighbors. For a node $v_i \in \mathcal{V}_P$ and its neighbors $\mathcal{N}(i)$, after attaching trigger g_i to node v_i, its neighbor can be divided into clean nodes $\mathcal{N}_c(i)$ and trigger nodes $\mathcal{N}_g(i)$. Then we can present the mathematical definition of IRT as follows:

$$\begin{aligned} \text{IRT} &= \frac{\#\text{Trigger Nodes in Top-k Important Nodes}}{\#\text{Poisoned Nodes } |\mathcal{V}_P|} \\ &= \frac{1}{|\mathcal{V}_P|} \cdot \sum_{v_i \in \mathcal{V}_{\mathcal{P}}} \frac{|\mathcal{N}_g(i)|}{|\mathcal{N}_g(i)| + |\mathcal{N}_c(i)|} \end{aligned} \tag{19}$$

As a fixed $\mathcal{V}_P$ makes $\frac{1}{|\mathcal{V}_P|}$ remains constant, the IRT value in our proof can be simplified as $\gamma = \sum_{v_k \in \mathcal{N}(g_i)} \alpha_{ik} = \frac{|\mathcal{N}_g(i)|}{|\mathcal{N}_g(i)| + |\mathcal{N}_c(i)|}$. Substitute γ with Eq.(18), we have:

$$\begin{aligned} \mathbb{E}[\mathbf{h}_i] &= (1-\gamma)\mathbf{W}\mathbb{E}_{\mathbf{x}\sim F_{y_i}}[\mathbf{x}] + \gamma \mathbf{W}\mathbb{E}_{\mathbf{x}\sim F_{y_t}}[\mathbf{x}] \\ &= (1-\gamma)\mathbf{W}\mu_{y_i} + \gamma \mathbf{W}\mu_{y_t} \end{aligned} \tag{20}$$

Let $\tilde{\mu}_y = \mathbf{W}\mu_y$ denote the class centroid feature vector in the embedding space via the linear mapping by a GNN model's weight matrix $\mathbf{W}$. To get a bound for the distance between $\mathbb{E}[\mathbf{h}_i]$ and $\tilde{\mu}_{y_t}$ in the embedding space, we substitute Eq.(20) with the triangle inequality and have:

$$\begin{aligned} \|\mathbb{E}[\mathbf{h}_i] - \tilde{\mu}_{y_t}\|_2 &= |\mathbb{E}[\mathbf{h}_i] - \tilde{\mu}_{y_i} + \tilde{\mu}_{y_i} - \tilde{\mu}_{y_t}\|_2 \\ &\geq \|\tilde{\mu}_{y_i} - \tilde{\mu}_{y_t}\|_2 - \|\mathbb{E}[\mathbf{h}_i] - \tilde{\mu}_{y_i}\|_2 \\ &= \|\tilde{\mu}_{y_i} - \tilde{\mu}_{y_t}\|_2 - \gamma\|\tilde{\mu}_{y_t} - \tilde{\mu}_{y_i}\|_2 \\ &\geq (1-\gamma) \cdot \|\tilde{\mu}_{y_t} - \tilde{\mu}_{y_i}\|_2 \end{aligned} \tag{21}$$

Following Wang & Shen (2024), we consider that the decision boundary in the embedding space for an arbitrary GNN model to predict node v_i as y_i is $\|\mathbf{h}_i - \tilde{\mu}_{y_i}\|_2 < \|\mathbf{h}_i - \tilde{\mu}_{y_j}\|_2, \forall y_i \neq y_j$. For a successful backdoor attack, there must have a small $\epsilon > 0$ such that $\|\mathbf{h}_i - \tilde{\mu}_{y_t}\|_2 < \epsilon < \|\mathbf{h}_i - \tilde{\mu}_{y_i}\|_2$. Substitute the equation with triangle inequality, we have:

$$\begin{aligned} \|\mathbf{h}_i - \mathbb{E}[\mathbf{h}_i]\|_2 &\geq \|\mathbb{E}[\mathbf{h}_i] - \tilde{\mu}_{y_t}\|_2 - \|\mathbf{h}_i - \tilde{\mu}_{y_t}\|_2 \\ &\geq \|\mathbb{E}[\mathbf{h}_i] - \tilde{\mu}_{y_t}\|_2 - \epsilon \end{aligned} \tag{22}$$

which indicates the successful backdoor attack is included in the bounds for $\mathbf{h}_i$ deviates from its expectation $\mathbb{E}[\mathbf{h}_i]$.

To continue the proof, we then introduce the celebrated Hoeffding's Inequality:

Lemma 1. (Hoeffding's Inequality). *Let $X_1, \ldots, X_n$ be independent bounded random variables with $X_i \in [a, b]$ for all i, where $-\infty < a \leq b < \infty$. Then*

$$\mathbb{P}\left(\frac{1}{n}\sum_{i=1}^{n}(X_i - \mathbb{E}[X_i]) \geq t\right) \leq \exp\left(-\frac{2nt^2}{(b-a)^2}\right) \tag{23}$$

and

$$\mathbb{P}\left(\frac{1}{n}\sum_{i=1}^{n}(X_i - \mathbb{E}[X_i]) \leq -t\right) \leq \exp\left(-\frac{2nt^2}{(b-a)^2}\right) \tag{24}$$

holds for all $t \geq 0$.

For each feature dimension $j \in \{1, ..., d\}$, the node embedding $\mathbf{h}_i$ can be decomposed as $\mathbf{h}_i[j] = \sum_{k \in \mathcal{N}(i)} \alpha_{ik} \mathbf{W} \mathbf{x}_k[j]$. For any dimension j, $\mathbf{x}_k[j]$ is independent and bounded by $[-S, S]$. Hence, directly use Hoeffding's inequality, for any $t_1 > 0$ and a fixed dimension j, we have:

$$\begin{aligned} \mathbb{P}\left(|\mathbf{h}_i(j) - \mathbb{E}[\mathbf{h}_i(j)]| \geq t_1\right) &\leq 2\exp\left(-\frac{2t_1^2}{\sum_k (2\alpha_{ik}\mathbf{W}S)^2}\right) \\ &\leq 2\exp\left(-\frac{\deg_i \cdot t_1^2}{2\rho(\mathbf{W})^2 S^2}\right), \end{aligned} \tag{25}$$

where $\rho^2(\mathbf{W})$ denotes the largest singular value of $\mathbf{W}$. By applying union bound over all d dimension, we extend Eq.(25) as:

$$\begin{aligned} \mathbb{P}\left(\|\mathbf{h}_i - \mathbb{E}[\mathbf{h}_i]\|_2 \geq t_1\sqrt{d}\right) &\leq \mathbb{P}\left(\bigcup_{j=1}^{d}\{|\mathbf{h}_i(j) - \mathbb{E}[\mathbf{h}_i(j)]| \geq t_1\}\right) \\ &\leq \sum_{j=1}^{d} \mathbb{P}\left(|\mathbf{h}_i(j) - \mathbb{E}[\mathbf{h}_i(j)]| \geq t_1\right) \\ &\leq 2d\exp\left(-\frac{t_1^2}{2\rho(\mathbf{W})^2 S^2 \cdot \frac{1}{\deg_i}}\right) \\ &= 2d\exp\left(-\frac{\deg_i t_1^2}{2\rho(\mathbf{W})^2 S^2}\right) \end{aligned} \tag{26}$$

Let $t_2 = t_1 \cdot \sqrt{d} = (1-\gamma) \cdot \|\tilde{\mu}_{y_t} - \tilde{\mu}_{y_i}\|_2$, then we have:

$$\begin{aligned} \mathbb{P}\left(\|\mathbf{h}_i - \mathbb{E}[\mathbf{h}_i]\|_2 \geq t_2\right) &\leq 2d\exp\left(-\frac{\deg_i t_1^2}{2\rho(\mathbf{W})^2 S^2 d}\right) \\ &= 2d\exp\left(-\frac{\deg_i \cdot (1-\gamma)^2 \cdot \|\tilde{\mu}_{y_t} - \tilde{\mu}_{y_i}\|_2^2}{2\rho(\mathbf{W})^2 S^2}\right) \end{aligned} \tag{27}$$

Substitute Eq.(27) with the upper bound of probability derived from Eq.(22), we denote $\rho(\mathbf{W}) = \|\mathbf{W}\|_2$ to present the matrix 2-norm of $\mathbf{W}$, then we have:

$$\begin{aligned}
\mathbb{P}(f(v_i) = y_t) &\leq \mathbb{P}\left(\|\mathbf{h}_i - \mathbb{E}[\mathbf{h}_i]\|_2 \geq t\right) \\
&\leq 2d \exp\left(-\frac{\deg_i \|\mathbf{W}\mu_{y_t} - \mathbf{W}\mu_{y_i}\|_2^2}{2\rho(\mathbf{W})^2 S^2 d}\right) \\
&\leq 2d \exp\left(-\frac{\deg_i \|\mathbf{W}\|_2 \|\mu_{y_t} - \mu_{y_i}\|_2^2}{2\rho(\mathbf{W})^2 S^2 d}\right) \\
&= 2d \exp\left(-\frac{\deg_i \|\mu_{y_t} - \mu_{y_i}\|_2^2}{2S^2 d}\right),
\end{aligned} \tag{28}$$

which completes the proof. □

I Additional Analysis of Attacking Against Adaptive Defenses

In Appendix A.7, we evaluated our method against existing defending strategies. While these widely adopted defending strategies highlight the effectiveness of BA-LOGIC, there are gaps between their defending goals and defending against logic poisoning.

Logic poisoning is a novel approach proposed by BA-LOGIC, which makes the trigger crucial for prediction by forcing a gradient-based importance score to exceed that of clean nodes, thereby directly increasing the probability of the victim model predicting the trigger-attached node as the target class without altering the label. We find that exploring the performance of BA-LOGIC against adaptive defenses, especially those designed to alleviate logic poisoning, could be informative.

In this subsection, we propose four adaptive defenses against logic poisoning attacks to further strengthen our contributions. Here, we present the brief introductions of these adaptive defenses. Specifically:

- **Explainability Regularization (ER)**: We leverage class activation mapping (CAM) Zhou et al. (2016) to measure the neighbors' contribution in predicting the target node. By incorporating an entropy-based regularization term during the training of the model, we penalize low-entropy CAM distributions on neighbors. This in-processing defense aims to avoid any single node becoming dominant for the prediction.
- **Gradient Masking (GM)**: We first train a victim model and record the neighbors' gradient contribution on the prediction of labeled nodes. A lower entropy implies high dependence on a certain neighbor, which might be the trigger node. Different from ER, GM is a pre-processing defense method. We mask out the edges between these nodes and obtain the cleaned graph.
- **Collaborative Defense (CD)**: We train a batch of independent GNNs with diverse initialization, data splits, and hyperparameters, then we adopt an ensemble aggregation to make a final prediction on nodes. As these independent models have various local prediction logic Deng & Mu (2023), the diverse prediction logic of collaborators can alleviate the logic poisoning.
- **Sampling And Masking (SAM)**: We repeatedly sample and mask edges during the training of the victim model. The edges are sampled from a probability distribution indicating the CAM-based importance for node prediction. Note that masking edges enables the model to perform masked forward propagation and update node representations, rather than clipping the edges. We use the before-and-after difference of the classifier in the final prediction as a regularization term to penalize when the prediction relies heavily on certain nodes.

We evaluate our BA-LOGIC and competitors against the proposed adaptive defense methods. We first finetuned these adaptive defenses based on the performance of defending against BA-LOGIC. We also record the clean accuracy of vanilla GNN models after applying the defenses with no attacks as **Accuracy**. Then we present the ASR|CA(%) of these methods in Tab. 18. The gray cell indicates the competitor with the highest ASR. From the table, we obtain the following key observations:

- The adaptive defense can partially weaken the backdoor, indicating promising directions against logic poisoning. However, under our BA-LOGIC, the ASR remains generally high, while CA

Table 18: Results (ASR|CA(%)) of backdoor methods against adaptive defenses.

Dataset	Defenses	Accuracy	ERBA	ECGBA	EBA-C	GTA-C	UGBA-C	DPGBA-C	BA-LOGIC
Cora	ER	84.11	7.83|82.36	42.59|82.07	20.74|75.75	30.56|82.38	45.82|80.37	49.31|82.91	**68.67|71.85**
	GM	84.12	6.91|73.71	52.31|75.58	19.38|67.10	31.42|73.73	50.41|71.16	51.16|74.94	**75.03|72.31**
	CD	84.10	0.05|74.72	44.62|78.14	21.78|68.11	45.34|74.74	62.71|70.14	48.10|76.45	**70.11|70.02**
	SAM	84.09	0.03|73.21	45.01|81.66	25.19|66.60	51.08|73.23	39.95|70.65	33.08|67.87	**59.29|75.69**
Pubmed	ER	86.51	5.12|80.57	52.17|86.18	17.53|80.38	27.68|80.98	46.11|74.75	57.09|80.16	**80.14|67.22**
	GM	86.51	3.21|75.65	56.22|80.01	16.29|75.46	28.45|76.06	52.30|71.16	52.61|75.16	**78.78|66.48**
	CD	86.49	0.13|77.08	54.41|81.55	14.68|76.89	21.37|77.49	64.51|72.24	51.11|76.85	**73.92|69.01**
	SAM	86.33	0.12|78.78	55.71|82.13	13.24|78.59	20.67|79.19	41.47|71.65	37.01|81.96	**77.15|66.23**
Flickr	ER	46.17	7.62|44.87	31.62|44.28	22.34|44.24	31.76|44.46	52.11|43.92	59.74|43.65	**69.02|41.27**
	GM	46.15	5.49|43.49	24.85|43.41	20.12|42.86	28.68|43.08	40.26|42.23	47.89|42.06	**75.49|39.84**
	CD	46.15	5.12|44.44	27.93|44.01	21.28|43.81	29.53|44.03	46.37|43.36	43.96|43.18	**82.93|40.52**
	SAM	46.04	4.38|43.67	26.71|43.12	19.85|43.04	27.83|43.26	43.05|42.66	40.18|42.47	**76.64|39.26**
Arxiv	ER	66.51	6.95|64.81	19.84|65.41	20.23|64.95	28.76|65.17	44.39|64.37	51.73|64.92	**59.68|61.83**
	GM	66.52	5.82|64.32	17.92|64.98	18.45|64.46	25.88|64.68	49.87|63.86	46.25|64.39	**72.96|60.97**
	CD	66.39	5.67|64.48	18.63|65.12	19.56|64.62	26.72|64.84	42.51|64.01	48.37|64.57	**65.11|62.34**
	SAM	66.21	5.21|64.02	18.21|64.73	19.12|64.16	27.15|64.38	40.94|63.52	47.06|64.08	**60.82|60.46**

significantly drops after applying adaptive defenses. This highlights the need for further in-depth investigation into adaptive defenses.

- Our method consistently maintains the highest ASR (generally over 60%) across adaptive defenses and datasets. This indicates the superiority of our BA-LOGIC in poisoning inner logic for clean-label backdoor.
- Our BA-LOGIC maintains the effective ASR-CA trade-off across datasets and various types of defenses. This highlights the challenge of fully cleansing the victim model, which already learns the poisoned prediction logic and relies on the injected triggers when predicting the poisoned nodes

J ADDITIONAL EMPIRICAL VALIDATIONS ON THEORETICAL ANALYSIS

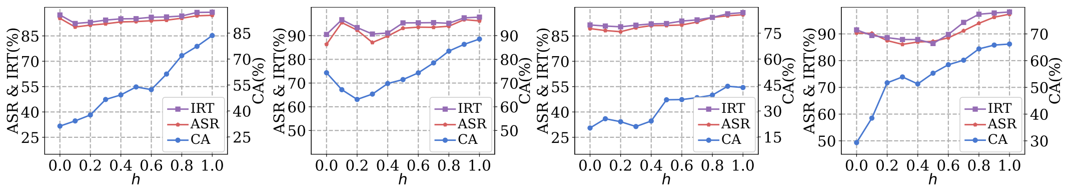

(a) Syn-Cora (b) Syn-Pubmed (c) Syn-Flickr (d) Syn-Arxiv

Figure 10: Performance of BA-LOGIC on synthetic graphs with different feature-label correlations.

In the main text of our work, we conducted a theoretical analysis to show that the core failure of existing methods under clean-label settings lies in that their triggers are deemed unimportant for prediction by GNN models. Specifically, we propose a novel metric, IRT, to measure the importance rate of triggers and establish a theoretical connection between IRT and attack success.

The theoretical analysis in Sec. 2.3 established the correlation between the IRT value and the probability of attack success. In this subsection, we aim to empirically investigate whether our theoretical analysis, i.e., the probability of attack success is bounded by the IRT value, still holds under various feature-label correlations from real-world graphs.

Inspired by Zhu et al. (2020), we use the **edge homophily** h, the fraction of edges in a graph that connect nodes that have the same labels, as a measure for the homophilous or heterophilous level of the feature-label correlation. To investigate how the homophilous and heterophilous correlations affect our method, we generate synthetic graphs based on **Cora**, **Pubmed**, **Flickr**, and **Arxiv** with various h. We illustrate the ASR|CA(%) and IRT(%) of BA-LOGIC on the synthetic graphs in Fig. 10.

From the figures, we obtain the following key insights:

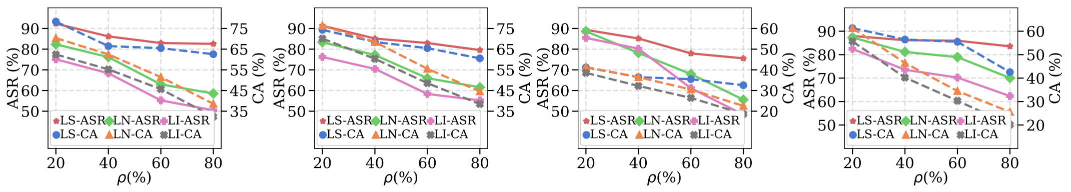

(a) Cora (b) Pubmed (c) Flickr (d) Arxiv

Figure 11: Performance of BA-LOGIC under sparse, noisy, and imbalanced label settings.

- ASR and IRT values are closely aligned for different h. It indicates that the theoretical analysis of triggers with a higher importance rate can achieve better attack performance remains valid for complex feature-structure correlations
- Our BA-LOGIC consistently achieves high ASR across datasets with various h. This indicates logic poisoning remains effective, facing complex feature-label correlations, as the GNN with poisoned prediction logic still identifies our trigger as important for prediction
- CA changes significantly with varying h. It is consistent with observations from prior works that homophily mainly affects the generalization of GNNs on clean nodes.

K ADDITIONAL ANALYSIS ON GENERALIZABILITY UNDER CHALLENGE SETTINGS

In the main text of our work, we evaluated our method across various graphs and target models. To further assess the generalizability of our method, here we systematically evaluate BA-LOGIC under five challenging yet realistic settings.

K.1 GENERALIZABILITY TO SPARSE, NOISY, AND IMBALANCED LABELS

In real-world graphs, supervision can be incomplete or corrupted, which may challenge the adaptive poisoned node selection strategy. To investigate the selection strategy and performance of BA-LOGIC with low-quality supervision, we propose three challenging settings of labels, specifically:

- **Label Sparsity (LS)**: We randomly mask a ratio of labels across all training nodes, and then retrain the poisoned node selector to obtain a new set of poisoned nodes.
- **Label Noise (LN)**: We randomly flip a ratio of labels of training nodes to other classes to simulate bad annotations, and then retrain the poisoned node selector to obtain a new set of poisoned nodes.
- **Label Imbalance (LI)**: We randomly mask a ratio of labeled nodes from the target class while keeping training nodes of other classes unchanged.

For each setting, we report (i) ASR and CA(%) of our method and (ii) the Jaccard overlap between the original set of poisoned nodes and the set selected under various challenging settings. We illustrate the results across four graphs in Fig. 11 and Fig. 12 for the performance and the overlap, respectively. From the figures, we have the following key findings:

- These supervision perturbations consistently degrade ASR and CA across all four datasets. But it mainly affects the clean accuracy of GNN models rather than our method, as it retains high ASR while CA starts to drop significantly.
- The Jaccard overlap between the original set of poisoned nodes and the manipulated set decreases smoothly as labels become sparser or noisier. It indicates that the perturbations challenge the poisoned node selector, as it is a normal 2-layer GCN whose generalizability might be affected by the settings.
- Label sparsity is consistently less harmful than label noise and label imbalance, as both ASR and overlap stay higher under LS than LN or LI. It suggests that BA-LOGIC prefers fewer but more reliable labels over many corrupted ones.

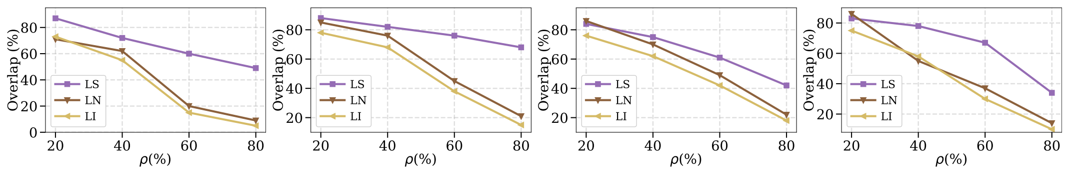

(a) Cora (b) Pubmed (c) Flickr (d) Arxiv

Figure 12: The Jaccard overlap of poisoned node selection under different label settings.

K.2 Generalizability to Noisy and Partially Accessible Features

Besides the challenge introduced by labels, the features of nodes in real-world graphs can be noisy or only partially accessible. To investigate the performance of Ba-Logic under degraded feature quality and accessibility, we further introduce two challenging settings of features, specifically:

- **Noisy Features (NF)**: We add dimension-wise Gaussian noise to node features before training Ba-Logic on the same graph, and vary the noise level to simulate different degrees of feature corruption.
- **Partially Accessible Features (PAF)**: We restrict the access to node features to only a part of the dimensions during the training of Ba-Logic, while the target GNN is still trained on the full feature space.

We first unify the perturbation ratios into normalized levels for the two settings, defined as:

$$\rho_{NF} = \frac{\sigma - \sigma_{\min}}{\sigma_{\max} - \sigma_{\min}}, \qquad \rho_{PAF} = 1 - \frac{d'}{d}, \tag{29}$$

where σ is the standard deviation of the injected Gaussian noise, $\sigma_{\min}$ and $\sigma_{\max}$ are the minimum and maximum noise levels used in our experiments, and $\frac{d'}{d}$ denotes the ratio of visible feature dimensions under the PAF setting.

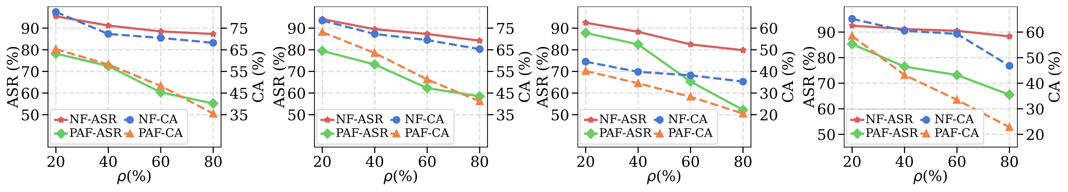

(a) Cora (b) Pubmed (c) Flickr (d) Arxiv

Figure 13: Performance of Ba-Logic under noisy and partially accessible feature settings.

We illustrate the results across four graphs with respect to ASR and CA(%) of our method in Fig. 13 with different noise levels and feature partials. From the figures, we have the following key findings:

- Increasing the feature perturbation level consistently degrades both ASR and CA across all four datasets. Our method retains high ASR, showing that logic poisoning remains effective even when feature quality deteriorates.
- NF mainly affects the GNN's CA, while PAF has a more significant impact on the ASR. It is consistent with the label noisy analysis, reflecting that the noise mainly affects the performance of GNNs rather than logic poisoning.

L Additional Time Complexity Analysis of Attacks and Defenses

In Appendix B, we conducted the time complexity of Ba-Logic. To highlight the efficiency of our method, we further present a comparison to competing graph backdoor methods in terms of time complexity. Let h denote the embedding dimensions, d denote the average degree of nodes in the graph, N denote the number of inner training iterations for the GNN model, $|\mathcal{V}|$ and $|\mathcal{V}_P|$ denote the size of poisoned nodes and training nodes, respectively. For clarity, we only keep the dominant terms with respect to the graph size, and present the analysis of the time complexity as follows:

- **ERBA**: The cost mainly comes from standard GNN training on the graph and injecting triggers into the $|\mathcal{V}_P|$ poisoned nodes for N GNN training iterations, leading to time complexity of $\mathcal{O}\big(dh(|\mathcal{V}| + N|\mathcal{V}_P|)\big)$.
- **ECGBA**: The method follows a bi-level optimization where a surrogate GNN and a single-node trigger generator are updated over N training iterations on the poisoned nodes, giving $\mathcal{O}\big(dh(|\mathcal{V}| + N|\mathcal{V}_P|)\big)$ time complexity.
- **EBA**: The method first leverages GNNExplainers to score nodes and then retrains the backdoored GNN, which also results in $\mathcal{O}\big(dh(|\mathcal{V}| + N|\mathcal{V}_P|)\big)$ time complexity.
- **GTA**: The cost mainly comes from a surrogate GNN and a trigger generator. Additionally, GTA coordinates an extra subgraph search around $|\mathcal{V}_P|$ nodes. The time complexity is approximate to $\mathcal{O}\big(dh\big((|\mathcal{V}| + (N+1)|\mathcal{V}_P|) + d^2\big)\big)$.
- **UGBA**: The method performs clustering-based poisoned node selection and a bi-level optimization on the whole graph, leading to $\mathcal{O}\big(dh(N+1)|\mathcal{V}|\big)$ time complexity.
- **DPGBA**: The method updates each outer iteration with both a surrogate GNN and a trigger generator. Additionally, DPGBA coordinates an OOD detector which needs N_o training iterations. The time complexity is $\mathcal{O}\big(dh\big(2|\mathcal{V}| + (N + N_o)|\mathcal{V}_P|\big)\big)$.
- **BA-LOGIC**: Our method optimizes a surrogate model and the logic poisoning trigger generator over N inner iterations, and the size of the trigger attached to $|\mathcal{V}_P|$ nodes is constrained by Δ_g. The time complexity is $\mathcal{O}\big(dh\big(2|\mathcal{V}| + (\Delta_g + N)|\mathcal{V}_P|\big)\big)$.

Based on the analysis, we present the comparison in Tab. 19.

Table 19: Time complexity comparison of attacks.

Methods	Time Complexity
ERBA	$\mathcal{O}\big(dh(\|\mathcal{V}\| + N\|\mathcal{V}_P\|)\big)$
ECGBA	$\mathcal{O}\big(dh(\|\mathcal{V}\| + N\|\mathcal{V}_P\|)\big)$
EBA	$\mathcal{O}\big(dh(\|\mathcal{V}\| + N\|\mathcal{V}_P\|)\big)$
GTA	$\mathcal{O}\big(dh\big((\|\mathcal{V}\| + (N+1)\|\mathcal{V}_P\|) + d^2\big)\big)$
UGBA	$\mathcal{O}\big(dh(N+1)\|\mathcal{V}\|\big)$
DPGBA	$\mathcal{O}\big(dh\big(2\|\mathcal{V}\| + (N + N_o)\|\mathcal{V}_P\|\big)\big)$
BA-LOGIC	$\mathcal{O}\big(dh\big(2\|\mathcal{V}\| + (\Delta_g + N)\|\mathcal{V}_P\|\big)\big)$

Additionally, we further give a comparison of the time complexity of defenses. Let L denote the number of layers of the GNN model. The complexity of training a GNN model mainly comes from aggregation with $\mathcal{O}(dh|\mathcal{V}|)$ and linear mapping with $\mathcal{O}(|\mathcal{V}|h^2)$. We first present the analysis of their time complexity as follows:

- **GCN-Prune**: Its time complexity mainly comes from computing feature similarities for all edges to identify low-similarity links, and then training an L-layer GNN on the pruned graph. It gives a time complexity of $\mathcal{O}\big(h|\mathcal{V}|L(d+h)\big)$.
- **RobustGCN**: The method performs robust message-passing and linear transformations on all nodes at each of the L layers. The edge-wise aggregation and node-wise feature update give a time complexity of $\mathcal{O}\big(h|\mathcal{V}|L(d+h)\big)$.
- **GNNGuard**: GNNGuard augments standard GNN training with a gating mechanism that assigns importance scores to neighbors and reweights message-passing along edges. The gating is implemented as an additional edge-wise operation on top of standard propagation. It gives a time complexity of $\mathcal{O}\big(h|\mathcal{V}|L(d+h)\big)$.
- **RIGBD**: RIGBD samples random edge-dropping masks and performs GNN propagation on each sampled graph to estimate the influence of edges. In each iteration, it draws K independent edge-dropping masks and runs L-layer GNN passes once on each masked graph, so the time complexity is $\mathcal{O}\big((K+1)h|\mathcal{V}|L(d+h)\big)$.

- **ER**: ER incorporates an explainability regularization term during training and computes neighbor contribution distributions over all C classes. Compared with standard GNN training, this introduces an additional multiplicative factor C, resulting in a time complexity of $\mathcal{O}\big(Ch|\mathcal{V}|L(d+h)\big)$.
- **GM**: GM first trains a victim model to obtain gradient-based neighbor contributions and then retrains on the graph where low-entropy edges are masked. It requires a dual L-layer GNN training on the whole graph, giving a time complexity of $\mathcal{O}\big(2h|\mathcal{V}|L(d+h)\big)$.
- **CD**: CD trains a batch of n independent GNN collaborators with diverse initialization, data splits, and hyperparameters, and aggregates their predictions. We formulate each collaborator with the same cost as a standard full-graph GNN, and the overall time complexity is $\mathcal{O}\big(nh|\mathcal{V}|L(d+h)\big)$.
- **SAM**: SAM repeatedly samples and masks edges according to CAM-based importance during training. In each iteration, the model performs a full pass and M additional masked passes, so the total cost is multiplied by $(M+1)$, resulting in a time complexity of $\mathcal{O}\big((M+1)h|\mathcal{V}|L(d+h)\big)$.

Table 20: Time complexity comparison of defenses.

Methods	Time Complexity
GCN-Prune	$\mathcal{O}(h\|\mathcal{V}\|L(d+h))$
RobustGCN	$\mathcal{O}(h\|\mathcal{V}\|L(d+h))$
GNNGuard	$\mathcal{O}(h\|\mathcal{V}\|L(d+h))$
RIGBD	$\mathcal{O}\big((K+1)h\|\mathcal{V}\|L(d+h)\big)$
ER	$\mathcal{O}(Ch\|\mathcal{V}\|L(d+h))$
GM	$\mathcal{O}(2h\|\mathcal{V}\|L(d+h))$
CD	$\mathcal{O}(nh\|\mathcal{V}\|L(d+h))$
SAM	$\mathcal{O}((M+1)h\|\mathcal{V}\|L(d+h))$

Here, we draw the following key observations from Tab. 19 and Tab. 20:

- The competitors and BA-LOGIC share similar linear time complexity in the graph size scaled by dh. For efficiency, BA-LOGIC only adds a $(\Delta_g + N)|\mathcal{V}_P|$ term for trigger generation, preserving the same order time complexity while achieving consistently higher ASR and comparable CA than competitors.
- Since $|\mathcal{V}_P| \ll |\mathcal{V}|$ and Δ_g is constrained by a small trigger size, the additional computation that BA-LOGIC requires for poisoning the inner prediction logic is modest relative to competitors. This renders the superior attack performance of BA-LOGIC a reasonable trade-off in terms of computational complexity.
- The adaptive defenses scale on training with additional multiplicative factors. While they reduce the ASR of graph backdoor attacks, they consistently cause significant CA drops, and BA-LOGIC remains more resilient than competing attacks. It implies that designing adaptive defenses that are both computationally efficient and effective against logic poisoning is still an underexplored research topic.